THE EFFECT OF RECUPERATOR GEOMETRY ON A REGENERATED BRAYTON CYCLE.

by

Barry Vaile Burrow

United States
Naval Postgraduate School

THESIS

THE EFFECT OF RECUPERATOR GEOMETRY

ON A REGENERATED BRAYTON CYCLE

by

Barry Vaile Burrow

June 1969

The Effect of Recuperator Geometry on a Regenerated Brayton Cycle

by

Barry Vaile Burrow
Lieutenant (junior grade), United States Navy
B. S., United States Naval Academy, 1968

Submitted in partial fulfillment of the
requirements for the degree of

MASTER OF SCIENCE IN MECHANICAL ENGINEERING

from the

NAVAL POSTGRADUATE SCHOOL
June 1969

ABSTRACT

A computer simulation of the Brayton cycle is used to develop a design procedure with respect to minimizing volume and weight for the counterflow plate-fin recuperator. Based on the Orenda OT-4 600 horsepower gas turbine, recuperator performance and dimensional characteristics are presented for an idealized equilateral plate-fin recuperator core matrix. The effects of plate spacings varying between 0.1 inches and 0.5 inches on recuperator performance characteristics are presented over a wide range of core frontal areas. Specific trends toward minimum volume and minimum weight plate-fin recuperator cores are discussed in detail.

TABLE OF CONTENTS

TABLES

ILLUSTRATIONS

NOMENCLATURE

English Letter Symbols

A	heat transfer area	sq ft
A_i	polynomial coefficient	
A_c	free flow area	sq ft
A_{fr}	frontal area	sq ft
a	plate thickness	ft
b	plate spacing	ft
c	recuperator width	ft
c_p	specific heat	BTU/(lbm deg F)
C	heat capacity rate	BTU/(hr deg F)
F	force	lbf
G	mass flow rate per unit area	lbm/(hr sq ft)
g	acceleration of gravity	(lbm ft)/(lbf sq sec)
h	convection heat transfer coefficient	BTU/(hr sq ft deg F)
HP	horsepower	hp
i	specific enthalpy	BTU/lbm
k	thermal conductivity	BTU/(hr sq ft deg F)/ft
L	flow length	ft
$\dot{m}$	mass flow rate	lbm/ft
P	pressure	lbf/sq ft
P_w	wetted perimeter	ft
q	heat transfer rate	BTU/hr
q_l	lower heating value of fuel	BTU/lbm

English Letter Symbols (continued)

r_h	hydraulic radius	ft
S	fin spacing	ft
s	specific entropy	BTU/(lbm deg R)
SFC	specific fuel consumption	lbm/(hp hr)
T	temperature	deg F, deg R
U	overall heat transfer coefficient	BTU/(hr sq ft deg F)
u	velocity	ft/sec
V	volume	cu ft
Vs	solid volume	cu ft
v	specific volume	cu ft/lbm
W_b	available shaft work	BTU/lbm
W_c	compressor work	BTU/lbm
Wt	mass	lbm
w	fin thickness parameter	ft

Greek Letter Symbols

α	ratio of total transfer area of one side of exchanger to total exchanger volume	sq ft/cu ft
β	compactness	sq ft/cu ft
δ	fin thickness	ft
ϵ	regenerator effectiveness	
θ	fin angle	deg
θ_o	temperature difference	deg F
μ	fluid viscosity	lbf hr/sq ft
ρ	density	lbm/cu ft
σ	ratio of free flow area to frontal area	sq ft/sq ft

Efficiency Terms

η_{comb}	combustor efficiency
η_c	compressor efficiency
η_f	fin effectiveness
η_{th}	thermal efficiency
η_t	turbine efficiency
η_o	surface effectiveness

Dimensionless Parameters

f	Fanning friction factor
j	Colburn-j factor
K_c	contraction loss coefficient
K_e	expansion loss coefficient
m	fin heat transfer parameter
NTU	Number of Transfer Units
Prel	relative pressure
$\frac{\Delta P}{P}$	relative pressure drop
Pr	Prandtl number
Re	Reynolds number
$r_{f/a}$	fuel to air ratio
St	Stanton number

ACKNOWLEDGEMENT

The author wishes to express his appreciation to Professor Paul F. Pucci for his continued assistance, encouragement, and particularly for his never ending good humor and geniality.

I. INTRODUCTION

The heat exchanger, a device which effects the transfer of heat from one fluid to another, is found whenever it is necessary to transfer energy without mixing the fluids involved. It is felt by many that our future as a power rich nation may depend partially on the heat exchanger engineer, as the most promising sources of power often present the most difficult applications. One such power source, the gas turbine, has a number of inherent advantages over the common gas and diesel engines; among them are compactness, low weight, ease of maintenance, and multi-fuel capabilities.

With the addition of a heat exchanger of reasonable size, the thermal efficiency of a gas turbine unit may be increased to about the same as, or slightly higher, than the gas engine [7].* The added weight of the exchanger, however, could well negate one of the primary advantages of the gas turbine. Furthermore, the relative rise in production cost due to the addition of a heat exchanger ought to be considered in any comparison, so as to keep the gas turbine on a specific cost level with the diesel engine.

Heat exchangers, however, are inherently bulky, heavy, and expensive. To overcome this problem, the concept of the compact heat exchanger has come into being. Not necessarily small, such an exchanger incorporates a heat transfer surface of high area density (leading to a high effectiveness for given weight and volume limitations) and, generally,

*Numbers in brackets designate references listed in Bibliography.

may be manufactured at a much lower cost per square foot of heat transfer area than the not so compact heat exchanger [9].

Although standard lines of compact heat exchangers have been adopted by many manufacturers, such exchangers may not be purchased as off-the-shelf items, as a proper design is needed for nearly every requirement. Such a design procedure usually considers the factors of heat transfer requirements, pressure drop characteristics, size, and cost, with an emphasis on the balance between the gain due to heat recovery and the loss due to pressure drop contributed by the addition of the exchanger.

There exist, however, numerous applications for which this much used design philosophy is not sufficient. Often the designer is faced with stringent volume or weight limitations. The technique of determining an optimized counterflow heat exchanger with respect to volumetric and weight considerations is developed in this study.

Fundamental relationships, assumptions, and design points upon which the investigation is based are presented in Sections II through IV; the computer program used to simulate the regenerated gas turbine cycle is discussed in Appendix B.

II. THE IDEAL REGENERATED BRAYTON CYCLE

The gas turbine plant, to a large extent, must have all its units designed with reference to the cycle on which it is to operate. The designer, therefore, must have a knowledge of the particular cycle to be considered. The most prevalent type of gas turbine in use today, the simple open cycle, has achieved great success due to its versatility [6]. With the addition of regeneration the efficiency of this cycle may be greatly increased.

The Brayton cycle, the basic thermodynamic cycle of the gas turbine, (refer to Figure 1) is characterized by taking air, as the working fluid, from the atmosphere into a compressor where part of the turbine power is used to raise the pressure before the air enters the cold side of a recuperator. The recuperator reduces the heat input to the cycle by transferring heat from the hot turbine exhaust gases to the cooler air. A further temperature increase occurs as fuel is burned directly in the air flow (forming gaseous products) through the combustor. The gas then enters a turbine, where it expands to a lower pressure while releasing energy available for work. Upon leaving the turbine stage, the gas enters the recuperator hot side and transfers much of its otherwise waste heat to the incoming air, before being exhausted into the atmosphere.

The particular cycle used in this heat exchanger investigation is based on the Orenda OT-4 gas turbine, a 600 horsepower unit engineered for the U. S. Navy [10]. The design specifications for the Orenda unit are:

HP	net power output	600 hp
η_{th}	overall thermal efficiency	34%
P1	compressor inlet pressure	2120 lbf/sq ft
T1	compressor inlet temperature	560 deg R
T4	turbine inlet temperature	2200 deg R
P6	exchanger exhaust pressure	2120 lbf/sq ft
P2/P1	compressor pressure ratio	4.0
$\frac{P3 - P4}{P3}$	combustor relative pressure drop	0.02
η_c	compressor efficiency	86%
η_{comb}	combustor efficiency	98%
η_t	turbine efficiency	86%
T_f	fuel inlet temperature	530 deg R
q_1	fuel lower heating value	19000 BTU/lbm

Other parameters which are usually specified for the cycle, such as the mass flow rate, regenerator effectiveness, and exchanger pressure drops, are not presented; they are, in fact, considered as variables in the optimization procedure to be discussed.

A more detailed discussion of the Brayton cycle is outlined in Appendix A.

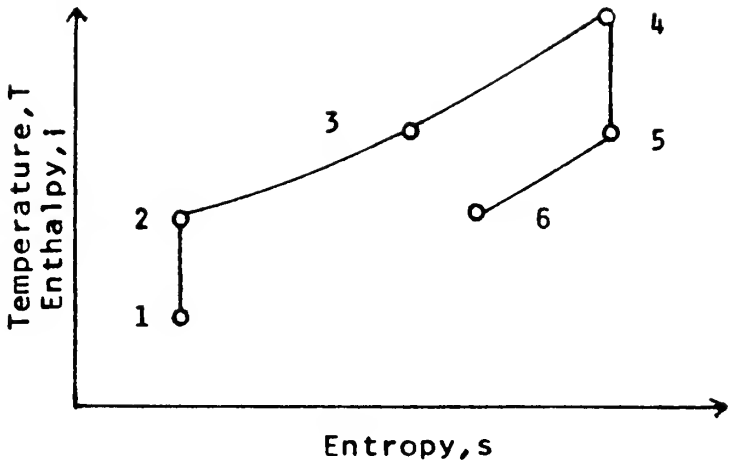

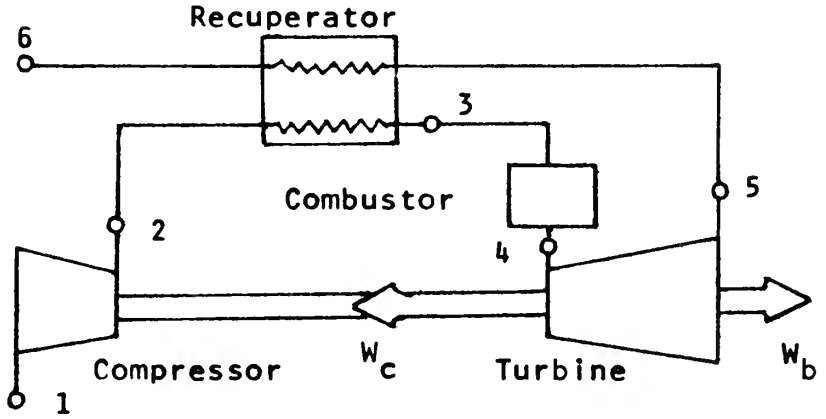

FIGURE 1 THE IDEAL REGENERATED BRAYTON CYCLE

III. RECUPERATOR SURFACE AND CORE GEOMETRY

For all applications in which the turbine inlet temperature is limited and a low to moderate pressure ratio is to be used, the most efficient method of improving the economy of the gas turbine involves the use of a heat exchanger, in which hot turbine exhaust gases give up heat to the relatively cool air from the compressor. Two basic heat exchanger models, the recuperator and regenerator, are in common use. The term recuperator (which is considered in this study) is usually applied to a continuous flow method of heat exchange, while the term regenerator specifies a periodic flow device, usually involving a moving matrix.

A. COMPACT HEAT EXCHANGERS

Considerations involving heat transfer characteristics of the gas turbine recuperative unit have led to the development of the compact heat exchanger. The term compact does not refer directly to a small bulk or weight, but to the heat transfer surface density of the exchanger. The most useful measure of this density is the compactness, β, where

$$\beta = \frac{\text{total transfer area of one side of exchanger}}{\text{volume between the plates of the same side}}$$

Somewhat arbitrarily, the working limits of compactness for a simple counterflow recuperator may be specified as 1000 sq ft/cu ft as the maximum working limit, and 200 sq ft/cu ft as the minimum limit before leaving the realm of compactness [9].

An understanding of the geometric parameters, presented in Figure 2, and subsequent relations most often used is essential to any compact heat exchanger design procedure.

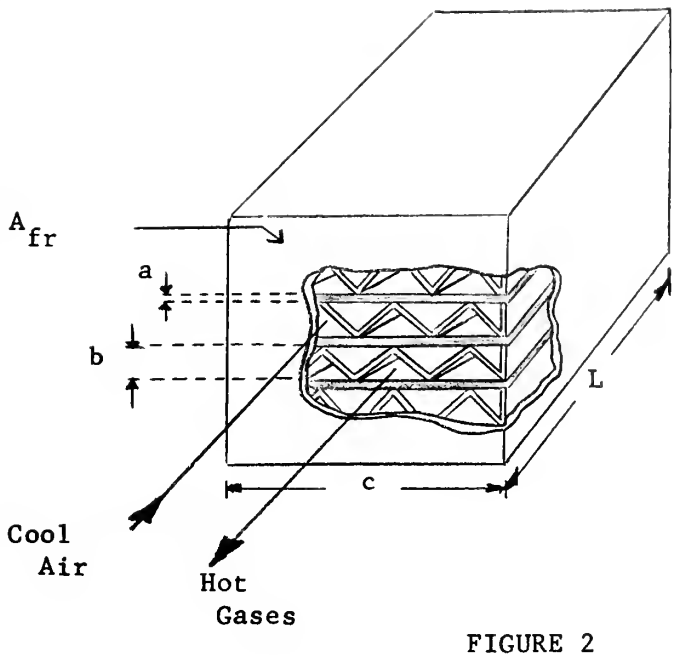

FIGURE 2

COMPACT COUNTERFLOW RECUPERATOR CORE

a	plate thickness	ft
b	plate spacing	ft
c	recuperator width	ft
r_h	flow passage hydraulic radius	ft
β	compactness	sq ft/cu ft
A	heat transfer area of one side	sq ft
A_c	free flow area of one side	sq ft
A_{fr}	frontal area	sq ft
L	flow length	ft
V	volume	cu ft
V_s	solid core volume	cu ft
α	ratio of total heat transfer area of one side to the total exchanger volume	sq ft/cu ft
σ	ratio of free flow area of one side to frontal area	dimensionless

The following equations give the relations between surface and core factors for one side of the counterflow plate-fin recuperator. Subscript 1 refers to any one side, and 2 refers to the other side. Factors without a subscript are common to both sides.

$$\beta_1 = \frac{A_1}{V_1} = \frac{A_1}{b_1 L c} \qquad 3.1$$

$$r_{h1} = \left[\frac{L A_c}{A} \right]_1 \qquad 3.2$$

$$\alpha_1 = \frac{A_1}{V} = \frac{b_1 \beta_1}{b_1 + b_2 + 2a} \qquad 3.3$$

$$\sigma_1 = \frac{A_{c1}}{A_{fr}} = \frac{A_1 r_{h1}}{L A_{fr}} = \alpha_1 r_{h1} = \frac{r_{h1} b_1 \beta_1}{b_1 + b_2 + 2a} \qquad 3.4$$

$$A_{c1} = \sigma_1 A_{fr} = \frac{A_1 r_{h1}}{L} \qquad 3.5$$

$$A_1 = \alpha_1 L A_{fr} \qquad 3.6$$

$$V_s = L\left[(A_{fr}) - (A_{c1} + A_{c2}) \right] \qquad 3.7$$

Among the factors common to both sides is A_{fr}, the total recuperator frontal area. The preceding relations are sometimes written on the basis that, for the counterflow recuperator, the hot and cold side

frontal areas are defined separately such that their sum equals A_{fr}. This investigation requires no such separation of terms and is based on the interpretation of frontal area as presented in Figure 2.

B. PLATE - FIN SURFACES

1. General Theory

Although other matrix forms are used, the plate-fin recuperator matrix is the most common [6]. Not only does this type of structure lend itself to light weight, extremely compact designs, but the plate spacing on each side may be easily optimized independently, allowing for design flexibility.

An understanding of the specific geometric parameters of the plate-fin matrix (Figure 3) and their relations is necessary to the design procedure.

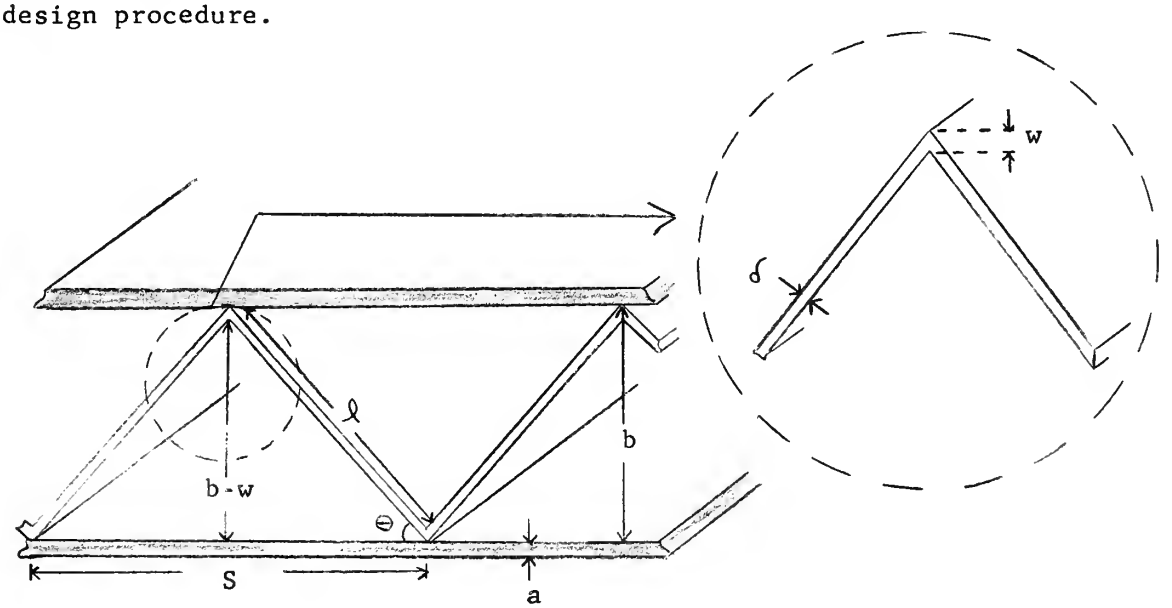

FIGURE 3

PLATE - FIN GEOMETRY

a	plate thickness	ft
b	plate spacing	ft
δ	fin thickness	ft
S	fin spacing	ft
A	heat transfer area	sq ft
A_c	free flow area	sq ft
P_w	wetted perimeter	ft
L	recuperator length	ft
w	fin thickness parameter	ft

$$S = \frac{2(b-w)}{\tan\theta} \qquad 3.8$$

$$A_c = \frac{1}{2} S(b-w) \qquad 3.9$$

$$P_w = 2l + S = 2\left(\frac{S}{2\cos\theta}\right) + S = S\left(\frac{1}{\cos\theta} + 1\right) \qquad 3.10$$

$$A = P_w L \qquad 3.11$$

From these relationships, the values for two very important parameters may be found.

$$r_h = \frac{A_c}{P_w} = (b-w)\left[2\left(\frac{1}{\cos\theta} + 1\right)\right]^{-1} \qquad 3.12$$

$$\beta = A\left[\left(\frac{1}{2} b \delta\right) L\right]^{-1} = \frac{2P_w}{b\delta} = \frac{2\left(\frac{1}{\cos\theta} + 1\right)}{b} \qquad 3.13$$

Since the recuperator matrix studied involves a fin angle, θ, of sixty degrees (resulting in an equilateral fin matrix) a further simplification may be made.

$$w = 2\delta \qquad 3.14$$

$$r_h = \frac{(b - 2\delta)}{6} \qquad 3.15$$

$$\beta = \frac{6}{b} \qquad 3.16$$

Table I represents values of these parameters for the plate spacings investigated. Although the spacings greater than 0.4 inches fall out of the previously defined compactness region ($200 \leq \beta \leq 1000$), they are included in the study since: (1) this region is arbitrary and (2) recuperator trends in weight and volume are more easily observed when large and small spacings are compared.

2. Specific Parameters

In order to keep the investigation on a common basis, all cores analyzed are assumed to be constructed of stainless steel, with constant properties, and uniform plate and fin thicknesses. The constant parameters used in the analysis are:

a	plate thickness	0.0008333 ft (0.01 in)
δ	fin thickness	0.0004166 ft (0.005 in)

k_f	thermal conductivity of stainless steel plates and fins	12 BTU/(hr sq ft deg F)/ ft
ρ_f	density of stainless steel plates and fins	484 lbm/cu ft

TABLE I

EQUILATERAL PLATE - FIN SPACINGS

Plate Spacing, b (in)	Compactness, β (sq ft/cu ft)	Hydraulic Radius, r_h * (ft)
0.1	720.00	0.0012500
0.125	576.00	0.0015972
0.15	480.00	0.0019444
0.175	411.43	0.0022917
0.2	360.00	0.0026389
0.25	288.00	0.0033333
0.3	240.00	0.0040278
0.35	205.71	0.0047222
0.4	180.00	0.0054167
0.5	144.00	0.0068056

* The hydraulic radius, r_h, is based on a fin thickness, δ, of 0.005 in.

IV. HEAT TRANSFER AND FLOW-FRICTION DESIGN THEORY

The design of a recuperator involves a consideration of both the heat transfer rates between the fluids and the pumping power expended to overcome fluid friction in the exchanger [8]. Obviously, one of the most desirable characteristics of a compact heat exchanger is that it yield a maximum heat exchange for a minimum pressure drop.

A. HEAT TRANSFER CHARACTERISTICS

Elementary heat transfer principles show that the cool air and hot gas flows should be in opposite directions; otherwise, the two streams would approach their mean temperature only. Subsequently, many compact heat exchangers involve a counterflow design, with plate-fin construction for added efficiency [5].

An overall heat transfer rate equation which includes convective and conductive heat mechanisms responsible for the heat transfer from the hot gases to the cool air may be written for a differential element as

$$dq = U\, dA\, (T_h - T_c) \qquad 4.1$$

where U is an overall heat transfer coefficient, dA represents an element of heat transfer area, and dq is a differential heat flux. A physical understanding of the heat transfer performance of the heat exchanger may be attained with the use of equation 4.1 and a number of parameters to be defined.

1. Fin Effectiveness

The straight recuperator fin of constant thickness δ and

length ℓ is represented in Figure 4. Such a fin extends from the base plate, at temperature T_0, through the moving fluid, at temperature T_∞, to a second plate. As there is no heat flux through the fin midway between the plates (due to the symmetry involved), a heat transfer analysis need only consider a fin of effective length $\ell/2$, insulated at the tip (Figure 4). An energy balance over an element of this fin [2] results in the equation:

$$q = k\, m\, A_f\, \Theta_o\, \mathrm{Tanh}(m\, \frac{\ell}{2}) \qquad 4.2$$

k = thermal conductivity of fin material

$m \approx \sqrt{\frac{2h}{k\delta}}$ = a dimensionless parameter for thin fins

$A_f \approx \delta(1)$ = cross section area of fin per unit width

$\Theta_o = T_0 - T_\infty$

h = convective heat transfer coefficient between the fin and the fluid

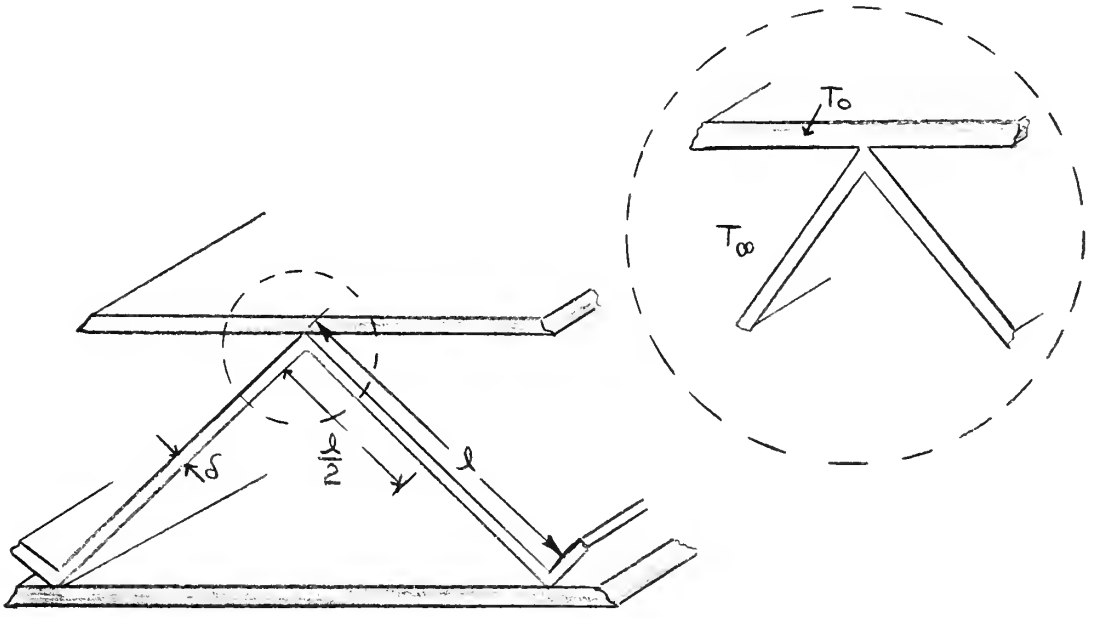

FIGURE 4

STRAIGHT FIN OF UNIFORM THICKNESS

In the order to express the heat exchanging capacity of an extended surface it is useful to define the term fin effectiveness as

η_f = fin effectiveness

$$\eta_f = \frac{\text{actual heat transferred from fin}}{\text{heat transferred if entire fin were at temperature } T_0}$$

$$\eta_f = \frac{k\, m\, A_f\, \Theta_o\, \text{Tanh}(m\, \ell/2)}{2\, L\, h\, (\ell/2)\Theta_o} \qquad 4.3$$

$$\eta_f = (\text{Tanh}(m\ \ell/2))\ (m\ \ell/2)^{-1} \qquad 4.4$$

2. Surface Effectiveness

Since the plate-fin geometry involves an array of fins, it is useful to define a total surface temperature effectiveness, η_o, which gives a measure of performance of the entire array. Defining "A" as the total heat transfer area of the combined fin and plate surfaces,

$$\eta_o = \frac{\text{actual heat transfer from A}}{\text{heat transfer if A were at } T_0} \qquad 4.5$$

$$\eta_o = \frac{(A - A_f)h(T_0 - T_\infty) + \eta_f\ A_f h(T_0 - T_\infty)}{A\ h\ (T_0 - T_\infty)} \qquad 4.6$$

$$\eta_o = 1 - \frac{A_f}{A}(1 - \eta_f)$$

3. Overall Heat Transfer Coefficient

The overall conductance U, as defined previously, may now be calculated as

$$U_c = \left[\frac{1}{(A_h/A_c)\eta_{o,h} h_h} + \frac{a}{(A_w/A_c)\, k} + \frac{1}{\eta_{o,c} h_c} \right]^{-1} \qquad 4.7$$

where U_c is based on a unit of cold side total surface [2]. In the

usual gas-to-gas recuperator, the second term in equation 4.7 (the wall resistance component) may be neglected relative to the fluid resistances.

$\eta_{o,h}$ $\eta_{o,c}$	overall surface effectiveness for hot and cold sides
A_w	average wall area
A_h A_c	total heat transfer area of hot and cold sides
h_h h_c	convection heat transfer coefficients of hot and cold sides
a	plate thickness
k	thermal conductivity of plate material

4. Counterflow Exchanger Heat Transfer Effectiveness

As previously stated, the most common and most effective flow arrangement for a two-fluid heat exchanger is the counterflow design. Referring to Figure 5, an energy balance leads to a second equation for the amount of heat transferred between the two fluids.

$$dq = (\dot{m} c_p)_h \, dT_h = (\dot{m} c_p)_c \, dT_c \qquad 4.8$$

Integration over the length of the recuperator leads to the equation

$$q = (\dot{m} c_p)_h (T_{h,in} - T_{h,out}) = (\dot{m} c_p)_c (T_{c,out} - T_{c,in}) \qquad 4.9$$

It is useful to define the term "capacity rate" as the product of the specific heat of one fluid and the mass flow rate of that fluid, C_h referring to the hot gas, and C_c referring to the cooler air.

$$q = C_h (T_{h,in} - T_{h,out}) = C_c (T_{c,out} - T_{c,in}) \qquad 4.10$$

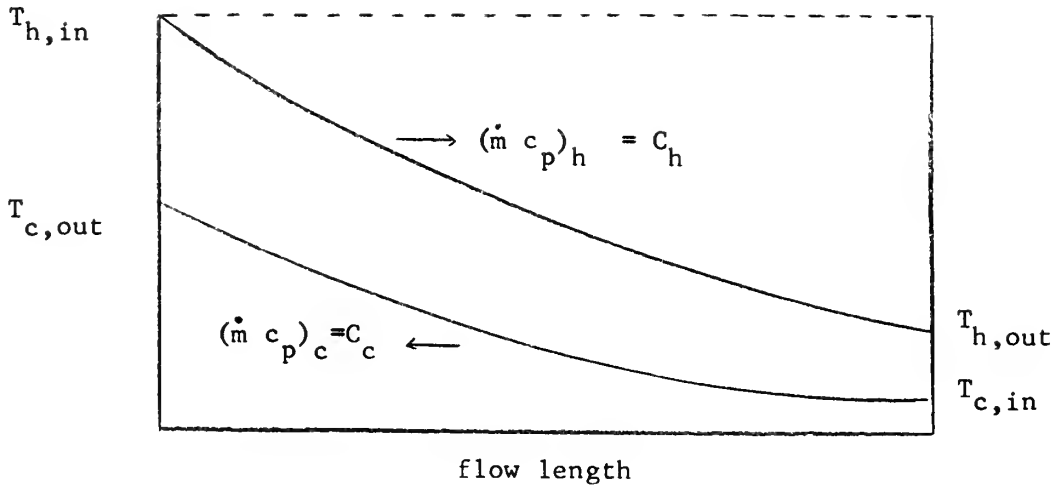

FIGURE 5

TEMPERATURE VARIATIONS IN COUNTERFLOW HEAT EXCHANGER

The heat transfer performance of the recuperator may now be determined by the heat exchanger effectiveness, ϵ , defined as the ratio of the actual heat transfer to the thermodynamic maximum heat transfer rate. The maximum heat transfer would be obtained if one of the fluids were to undergo a temperature change equal to $(T_{h,in} - T_{c,in})$, the maximum temperature difference in the counterflow exchanger. Since the heat lost by the hot gas must be gained by the cooler air (neglecting losses), as may be seen in Equations 4.9 and 4.10, the fluid undergoing this maximum temperature change must have the lower of the two capacity rate values, C_{min}.

$$q_{max} = C_{min}(T_{h,in} - T_{c,in}) \qquad 4.11$$

The effectiveness may now be determined as

$$\epsilon = \frac{\text{actual heat transfer}}{\text{maximum heat transfer}}$$

$$\epsilon = \frac{C_h(T_{h,in} - T_{h,out})}{C_{min}(T_{h,in} - T_{c,in})} = \frac{C_c(T_{c,out} - T_{c,in})}{C_{min}(T_{h,in} - T_{c,in})} \qquad 4.12$$

From the previous equations, the effectiveness may be shown to be independent of the fluid temperatures [2].

$$\epsilon = \frac{1 - e^{-(1 - \frac{C_{min}}{C_{max}})\frac{UA}{C_{min}}}}{1 - \frac{C_{min}}{C_{max}} e^{-(1 - \frac{C_{min}}{C_{max}})\frac{UA}{C_{min}}}} \qquad 4.13$$

where C_{min} and C_{max} are, respectively, the smaller and the larger of the two capacity rate magnitudes.

Finally, defining the Number of Transfer Units, NTU (a dimensionless expression for the heat transfer size of the recuperator), as the ratio of (U A) to C_{min}, where A refers to the total surface area on which U is based, the effectiveness may be written as

$$\epsilon = \frac{1 - e^{-(1 - \frac{C_{min}}{C_{max}})NTU}}{1 - \frac{C_{min}}{C_{max}} e^{-(1 - \frac{C_{min}}{C_{max}})NTU}} \qquad 4.14$$

A comparison of this equation with effectiveness relations for other geometries will lead to the conclusion that the counterflow arrangement is indeed useful for gas flow recuperators (for which $C_{min}/C_{max} \approx 1$) when an effectiveness in the order of 80% is to be obtained.

B. FLOW - FRICTION THEORY

In the design of a gas-to-gas heat exchanger, the pressure drop characteristics assume an importance equal to that of the heat transfer characteristics [8]. The designer is generally interested in the overall core pressure drop, including entrance and exit effects, rather than the core friction pressure drop alone.

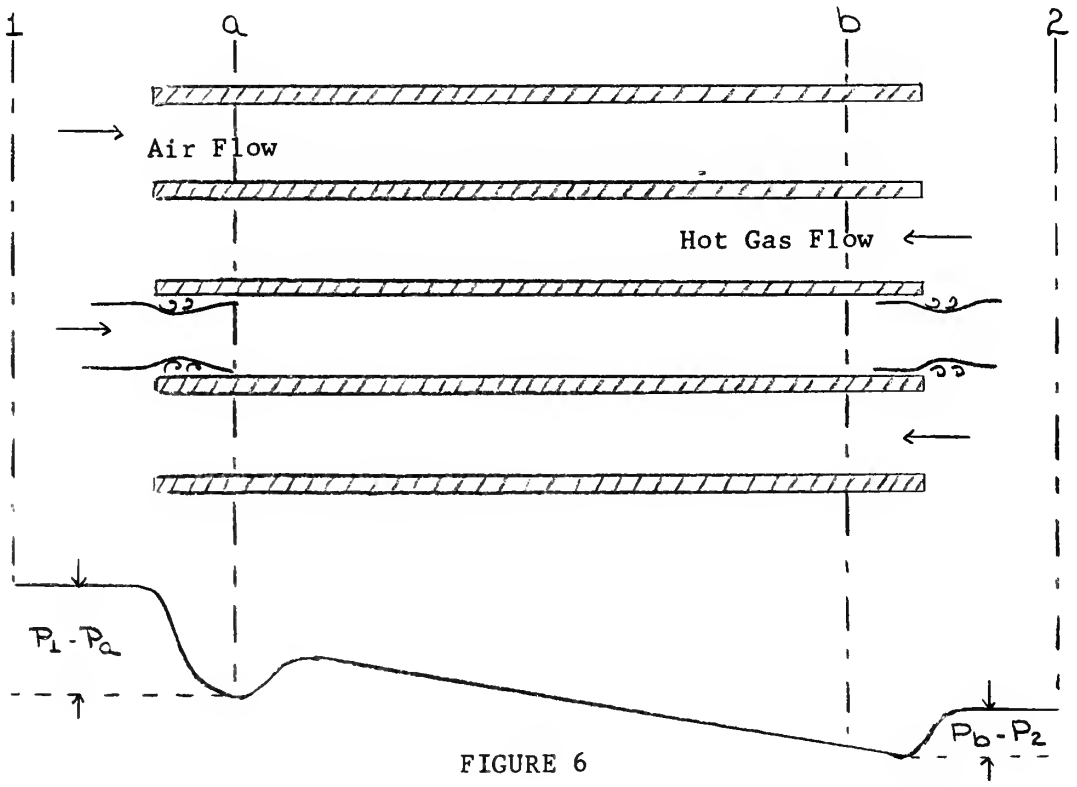

FIGURE 6

RECUPERATOR CORE MODEL FOR COOL AIR FLOW PRESSURE DROP ANALYSIS

1. Core Friction and Flow Acceleration

The core friction pressure loss term, due to viscous shear and pressure force, is expressed in terms of the dynamic head $\frac{\rho u^2}{2g}$, the appropriate friction factor, f, and the ratio of the length to hydraulic radius of one side, $\frac{L}{r_h} = \frac{A}{A_c}$, as

$$\Delta P_{friction} = f\left(\frac{A}{A_c}\right)\left(\frac{\rho_m u^2}{2g}\right) \qquad 4.15$$

$$\Delta P_{friction} = f\left(\frac{A}{A_c}\right)\left(\frac{G^2}{2g\rho_m}\right) \qquad 4.16$$

where G is based on the minimum free flow frontal area ($G = \rho_1 u_1 = \rho_2 u_2 = \frac{\dot{m}}{A_c}$) and ρ_m is the average core fluid density ($\rho_m = \frac{\rho_1 + \rho_2}{2}$).

Since density changes occur in the core as the fluid temperature changes, a term accounting for flow acceleration must be included in the pressure drop analysis. The change in momentum due to this fluid acceleration may be expressed as

$$\Delta P_{acceleration} = \frac{F}{A_c g} \qquad 4.17$$

$$\Delta P_{acceleration} = \frac{\dot{m}(u_b - u_a)}{A_c g} \qquad 4.18$$

$$\Delta P_{acceleration} = \frac{G^2}{g}\ \frac{1}{\rho_a}\left(\frac{\rho_a}{\rho_b} - 1\right) \qquad 4.19$$

2. Entrance and Exit Effects

The entrance pressure drop, due to the free flow area change as well as to the irreversible free expansion following the abrupt inlet contraction may be written as [8].

$$P_1 - P_a = \left(\frac{1}{2g}\right)\rho_1 u_1^2 (1 - \sigma^2) + \rho_1 K_c \frac{u_1^2}{2g} \qquad 4.20$$

$$P_1 - P_a = \frac{G^2}{2g\rho_1}\left(1 - \sigma^2 + K_c\right) \qquad 4.21$$

where a constant density is assumed to exist from point "1" to point "a'. K_c, the contraction, or entrance, coefficient may be calculated by methods explained in Ref. [8].

Similarly, the exit pressure rise is due to the change in flow area (which is identical to the corresponding entrance pressure drop term) and the irreversible free expansion and momentum changes following the abrupt exit expansion. This pressure rise is written as

$$P_b - P_2 = \left(\frac{1}{2g}\right) \rho_2 u_2^2 (\sigma^2 - 1) + \rho_2 K_e \frac{u_2^2}{2g} \qquad 4.22$$

$$P_b - P_2 = \frac{G^2}{2g\rho_2} (\sigma^2 - 1 + K_e) \qquad 4.23$$

where K_e, the exit coefficient, is evaluated in Ref. [8].

3. Overall Pressure Drop

The combination of all pressure drop effects results in the equation

$$P_1 - P_2 = \frac{G^2}{2g\rho_1}\left[(1 - \sigma^2 + K_c) + \frac{2\rho_1}{\rho_a}\left(\frac{\rho_a}{\rho_b} - 1\right) + \frac{\rho_1}{\rho_m} f \frac{A}{A_c} + \frac{\rho_1}{\rho_2}(\sigma^2 - 1 + K_e)\right] \qquad 4.24$$

As it has been assumed that $\rho_a \approx \rho_1$ and $\rho_b \approx \rho_2$ the relation for the overall exchanger pressure drop in terms of specific volume, where $v_m = \frac{v_1 + v_2}{2}$ may be written as

$$P_1 - P_2 = \frac{G^2 v_1}{2g}\left[(K_c + 1 - \sigma^2) + 2\left(\frac{v_2}{v_1} - 1\right) + f \frac{A}{A_c} \frac{v_m}{v_1} - \frac{v_2}{v_1}(1 - \sigma^2 - K_e)\right] \qquad 4.25$$

C. PARAMETRIC APPROXIMATIONS

In the preceding heat transfer and flow friction analysis, a number of important engineering parameters and fluid properties are used in fundamental relationships. Usually presented only in tabular or graphical form, these parameters may not be directly obtained in a computer analysis. To overcome this problem, functional relationships approximating the tabulated values must be made a part of the computer program.

For the program [1], such relationships were formulated by making a "least squares fit" of the curves representing tabulated data of the required parameters. The resulting functional relationships, of the form

$$P(x) = A_1 + A_2 x + A_3 x^2 + \ldots\ldots\ldots + A_i x^{i-1} \qquad 4.26$$

where: $P(x)$ = desired parameter

x = variable on which the parameter is based

A_i = polynomial coefficients resulting from least squares fit

$i-1$ = order of resulting polynomial

are used extensively in the computer analysis. Table II specifies the parameters for which such polynomial approximations are used, the variable on which each is based, and the order of the polynomial.

Table II indicates that two parameters for which functional relationships must be obtained are dependent on the Reynolds number, $\rho u (4r_h)/\mu$. The Fanning friction factor, f, is used in equation 4.15 and subsequent relations to obtain the pressure drop due to core friction through the recuperator. The Colburn-j factor, j, has been obtained experimentally

for a number of recuperator geometries [8] and is used to obtain the convection heat transfer coefficient, h, as follows:

This heat transfer parameter is defined as

$$j = St\ Pr^{2/3} \tag{4.27}$$

Since j and Pr are determined from functional relationships, the Stanton number may be calculated as

$$St = j\ Pr^{-2/3} \tag{4.28}$$

Thus, the convection heat transfer coefficient, used in equation 4.5 and subsequent relations, is obtained as

$$h = St\ c_p\ \rho\ u \tag{4.29}$$

Experimental investigations of f and j provide curves similar to those presented in Figure 7. As indicated, the laminar flow regime ($Re < 1000$) produces linear relationships for the ideal equilateral triangular passage such that

$$f = 13.33/Re \tag{4.30}$$

$$j = 2.64/Re \tag{4.31}$$

The turbulent region ($Re > 5000$) data may be closely approximated by the linear relationship resulting from circular tube flow as

$$f = 0.046\ Re^{-0.2} \tag{4.32}$$

$$j = 0.023\ Re^{-0.2} \tag{4.33}$$

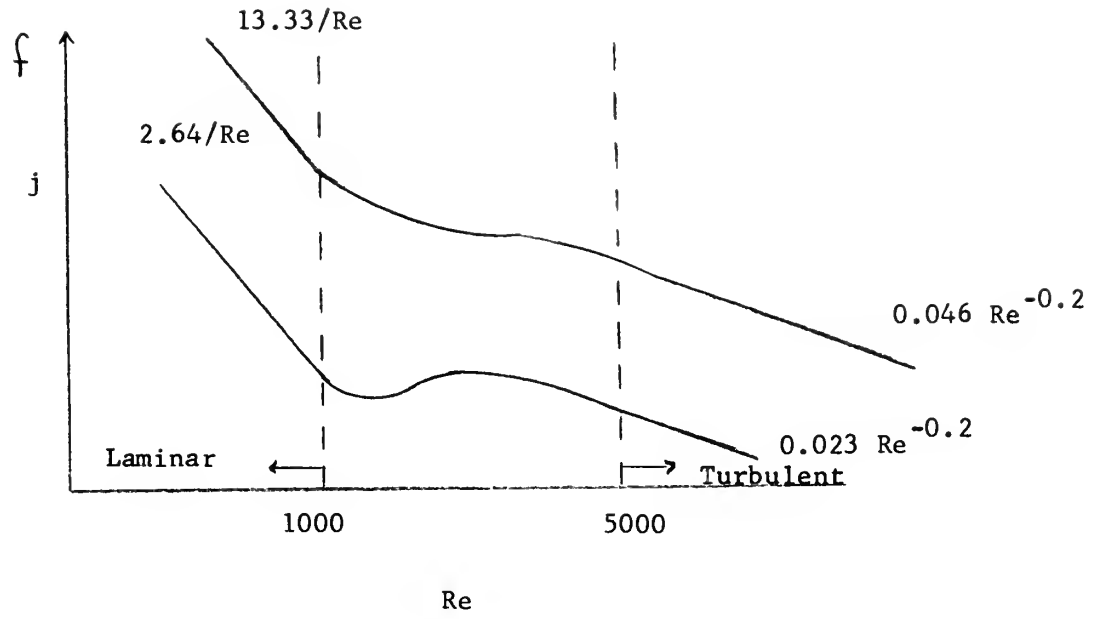

FIGURE 7

EXPERIMENTAL CURVES FOR f AND j

The transition region ($1000 \leq Re \leq 5000$) is also based on experimental data and must be approximated by a polynomial equation for computer analysis. The polynomial coefficients for the resulting equations approximating this transition region, as well as those for the other parameters in Table II, are presented in Appendix B.

TABLE II

FUNCTIONAL RELATIONSHIPS

	Parameter	Function Of	Order Of Polynomial
f	Fanning friction factor	Reynolds number	10
j	Colburn-j factor	Reynolds number	10
Pr	Prandtl number	temperature	9
μ	viscosity	temperature	9
c_p	specific heat	temperature	5
i	enthalpy	temperature	6
P_{rel}	relative pressure	temperature	8
T	temperature	relative pressure	8
T	temperature	enthalpy	9

V. RESULTS

A. OBJECTIVES

For many years engineers have designed heat exchangers by first assuming core dimensions and then calculating mass flow rates, heat transfer rates, and pressure drops which would occur if fluids were flowing through the assumed core. Extensive investigations of various heat transfer surfaces offer the designer enough latitude in surface geometry to successfully meet the heat transfer and pumping power requirements for a specific application.

Texts frequently refer to the possibility of optimizing the internal core dimensions of a heat exchanger once a particular surface is specified, yet very little research has been published in this area. Such a technique forms the basis for this study.

The computer program [1] used in the study simulates the open gas turbine regenerated cycle under constant load conditions. All adjustments in internal exchanger geometry are reflected directly in terms of the cycle thermal efficiency and the overall core size necessary to obtain that efficiency. As is outlined in Appendix C, any computer simulation of the gas turbine cycle requires set tolerance limits on various cycle design points which must be met. Early investigations of general recuperator trends in the study involved a tolerance limit of 3.3% for the desired thermal efficiency of 0.34 and a limit of 0.2% for the desired horsepower output of 600. More detailed analysis (as presented in Figures 15 through 22 and Tables V through VII) required tighter tolerances of 1.45% for the thermal efficiency and 0.09% for the horsepower. The use of two tolerance levels slightly affects output data for the same core, as may be noticed.

B. GENERAL RECUPERATOR CHARACTERISTICS

Trends in external dimensions of the plate-fin recuperator due to changes in internal spacings may be noted by investigating a number of different cores. A sufficient number of cores may be obtained by pairing the plate spacings presented in Table I. For convenience a particular core will be referred to in terms of the ordered pair (b_c, b_h) where b_c represents the cold side spacing and b_h represents the hot side spacing of the core.

Due to addition of fuel in the combustor, the mass flow rate through the recuperator hot side is larger than the cold side flow rate by a factor of the fuel to air ratio, $r_{f/a}$. The hot side mass flow rate must be accommodated, then, by an increase in fluid density, flow area, or fluid velocity ($\dot{m} = \rho A v$). Since fluid density decreases as temperature increases the engineer is left with only two alternatives.

A velocity increase will not only accommodate the increased mass flow rate, but it will also increase the heat transfer rate per unit of surface area by a factor something less than the first power of the velocity. The friction power expenditure, however, will increase by a factor between the square and the cube of the velocity [8]. It is this effect which serves as the basis for the design restriction that the hot side plate spacing never be less than the cold side spacing.

General recuperator volume trends may be noted in Figure 8 for five specific cores. Each point on every curve represents the external core dimensions which will satisfy the specified design points. As might be expected, from the definition of the compact heat exchanger, larger cores are required as one moves from the more compact to the larger spacings; for any one frontal area, more length, and thus more heat transfer area,

is required as spacings increase. Excluding the extremely compact core, (0.1, 0.1), points of minimum volume for each core fall below a frontal area of five square feet. Furthermore, every core requires a frontal area of at least two square feet before the specified cycle design points are met.

A more detailed view is presented in Table III, in which the minimum volume of the (0.1,0.1) core is seen to fall within a frontal area range between 30 and 40 square feet. Definitely, the minimum volume of such a core does not present the optimum package. Similar characteristics were noted only for two other extremely compact cores, (0.1, 0.125) and (0.125, 0.125).

An increase in length over a region of increasing frontal area is noticeable in all cores except those having a cold side spacing of 0.1 inches. Occurring at a frontal area greater than that for the minimum volume core, this effect becomes more apparent as core spacings increase. Table III indicates that the mass flow rates for these cores decrease as frontal area increases. Not shown is the fact that the recuperator hot and cold side Reynolds numbers also decrease with the mass flow rate. The first knee of each curve (that point at which L begins to increase with A_{fr}) occurs when the two Reynolds numbers approach a magnitude of 2000. Reference to Figure 7 indicates a decrease in the Colburn-j factor with decreasing Re at this point. Evidently, the resulting decrease in the convection heat transfer coefficient, h (which is proportional to j), is accompanied by an increase in heat transfer area (as L increases with A_{fr}) in order that the desired cycle thermal efficiency be maintained. This effect continues as j decreases until the second knee at which the two Reynolds numbers have approached a magnitude near 1000.

At this point, since j begins to increase with increasing frontal area, less heat transfer area is required, and L begins to decrease.

The effect is not noticeable for those cores of low plate spacings, as both the hot and cold side Reynolds numbers of such cores fall in the laminar region for all frontal areas. Reynolds numbers for cores of low cold side spacing and large hot side spacing (i.e., (0.1, 0.5)) however, tend to have a maximum Reynolds number near 2000 at low frontal areas, followed by a rapid drop as frontal area increases. The slight length increase required by such cores is not noticeable due to the magnitude of the length increments used at this point of the investigation.

Relative pressure drops on both sides of all cores decrease to zero as frontal areas increase. In the region of minimum volume ($A_{fr} < 5$ sq ft), the cold side relative pressure drop appears to be negligible for all cores except that which combines a small cold side spacing and a large hot side spacing. The hot side relative pressure drop, on the other hand, appears to be high only for those cores in which the two plate spacings are of equal magnitude.

C. MINIMUM VOLUME AND WEIGHT CORES

Figure 9 indicates dimensional requirements for various cores in the minimum volume region. As is to be expected, required lengths, and therefore volumes, increase as core spacings increase. The effect of forming cores of unequal spacings as compared to equally spaced cores is presented in Figure 10.

To this point a trend has developed in which smaller spacings require smaller cores. Based on this trend, one might incorrectly reason that the minimum volume for a given hot side spacing may be obtained simply by decreasing the cold side spacing to a minimum allowable magnitude. In fact, for the cores of 0.25 inch hot side spacing this appears

to be the case as b_c is reduced from 0.25 inches to 0.1 inches. However, the trend presented by those cores for which b_h is 0.5 inches as b_c decreases should be noted. A decrease from a cold side spacing of 0.5 inches to 0.25 inches reduces core volume; a further decrease to a b_c of 0.1 inches produces a core of extremely large volume. This core, which combines the large length and frontal area requirements of the two range limiting spacings, results in the largest minimum volume point recorded of all cores investigated.

Similar analysis shows the effect, presented in Figures 11 through 13, of increasing the hot side spacing for a constant b_c. For all cores presented, the b_h increase results in increased frontal area and length requirements; thus, the minimum volume for each series of constant cold side spacing cores increases as the hot side spacing is increased.

Recuperator dimensional and performance characteristics at minimum volume points are presented in Table IV ; each set of cores listed consists of a constant b_c with increasing b_h. The optimum core with respect to volume in each set occurs at or near that core configuration for which b_h is twice b_c. The optimum core with respect to weight for each set consists of the same, or a slightly higher, b_h as the optimum volume core. Such a trend might lead one to believe a rule of thumb often used by manufacturers that the core hot side spacing be twice the cold side spacing. Analysis will show this to be an inadequate design procedure. Further investigation in this area, however, should be preceded by mention of the performance characteristics of the minimum core points as tabulated in Table IV.

For any one set of cores, the cold side relative pressure drop increases with increased b_h, while the hot side relative pressure drop

decreases. This effect is presented graphically for one set of cores in Figure 14. The large magnitude of the hot side relative pressure drop for cores of $b_h \approx b_c$ is to be expected since the hot side mass flow rate must be accommodated by an increase in either flow area or velocity over that of the cold side flow. Since there is little or no area increase ($b_h \approx b_c$), velocities on the hot side of such cores must be higher, yielding relatively large pressure drops. As mass flow rates generally fall and flow areas increase as b_h is increased for each set of cores, the hot side relative pressure drop falls. Evidently, the cold side relative pressure drop is affected more by the general length increase, as b_h increases for each set, than by the decreasing trend in the mass flow rate. Thus, the cold side relative pressure drop rises with b_h in each set of cores.

D. OPTIMUM CORES

Concentrating once again on dimensional aspects, Figures 15 through 19 represent the effect of increasing b_h for a constant b_c in the region of optimum core spacings with respect to volume and weight. It is apparent from these plots that an optimum design procedure is not that for which $b_h = 2b_c$. Tables V and VI present the characteristics of cores optimized with respect to volume and weight; Table VII, which consists of performance data for cores of $b_h = 2b_c$, is presented for comparison. A comparison of Tables V and VI indicates that the minimum volume core for any one b_c involves a higher mass flow rate and less length than the corresponding minimum weight core. This results in a lower cold side and higher hot side relative pressure drop through the minimum volume core as compared to the minimum weight core for any set b_c.

Further investigation of the Tables indicates that the minimum weight core for any b_c requires a larger b_h than that for the minimum volume core. This effect (noticed earlier in Table IV) is to be expected, as the minimum weight core represents a compromise between a low core volume and a low overall core density (which decreases as spacings increase). Differences between the two sets of optimized cores and those cores for which $b_h = 2b_c$ are illustrated in Figure 20.

Allowing a tolerance limit of 0.004 inches either side of the optimum hot side spacing for any given cold side spacing as presented in Tables V and VI, smooth optimum spacing curves may be drawn, as shown. In the range of cold side spacings between 0.1 and 0.225 inches a linear relationship closely approximates each of the two optimum spacing curves, as

$$b_h = 0.86\, b_c + 0.12 \qquad (0.1 \leq b_c \leq 0.225) \qquad 5.1$$

for optimum volume spacings and

$$b_h = 1.16\, b_c + 0.12 \qquad (0.1 \leq b_c \leq 0.225) \qquad 5.2$$

for optimum weight spacings.

Outside this range of cold side spacings the optimum core plots tend to level off, thus tending to keep the cores within the limits of compactness of the compact heat exchanger region.

Since the engineer is usually at liberty to choose both plate spacings, he must have an idea of the relative volumes and weights between the optimum cores which he may use. Figure 21 presents volume characteristics of optimized cores from Table V with respect to the minimum volume core (0.125, 0.225). As may be seen, if the engineer expects to use a cold side spacing equal to or greater than 0.175 inches, he must accept

the fact that his optimum core will have a volume at least 20% greater than the minimum available. Similarly, Figure 22 represents the weight characteristics of cores from Table VI with respect to the minimum weight core of (0.175, 0.332). Although the variance in weight is not as great as that for volume, on a percentage basis, it may be seen that the engineer must expect weights at least 5% greater than the minimum available if he wishes to use cold side spacings other than those between 0.125 and 0.235 inches. The very large increase in relative weight as extremely compact cores ($b_c \leq$ 0.1 inches) are optimized should also be noted.

For the design points of this study, if the engineer were free to optimize any non-dimensional parameter (as mass flow rate or relative pressure drops) while keeping within 10% of the minimum volume possible, reference to Figure 21 and the use of equation 5-1 would indicate a freedom of b_c choice between 0.1 and 0.15 inches and b_h choice between 0.206 and 0.28 inches. A similar design procedure with a limit of 5% over the minimum weight core (using Figure 22 and equation 5-2) would yield a b_c range between 0.13 and 0.225 inches and a b_h range between 0.27 and 0.38 inches. A reference back to Table IV will indicate that the minimum weight and minimum volume cores for all cores investigated do fall within the indicated ranges of spacings. If both volume and weight of the core are limited within the specified 10% and 5%, the range of allowable cold side spacings is further reduced to between 0.13 and 0.15 inches, and the allowable hot side range to 0.27 to 0.28 inches.

Although the design limitations outlined are applicable only to the specific core geometry studied, the procedure may be applied to all similar geometries. As indicated, when core and weight tolerances are specified, the engineer does have some freedom in choosing internal core

dimensions based on other requirements. In all applications for which the allowable volume or weight of the gas turbine is at a premium, it seems that the engineer would be wise to follow a design procedure for the heat exchanger, as outlined, which optimizes the limited quantity, before moving on to further core optimization with respect to performance.

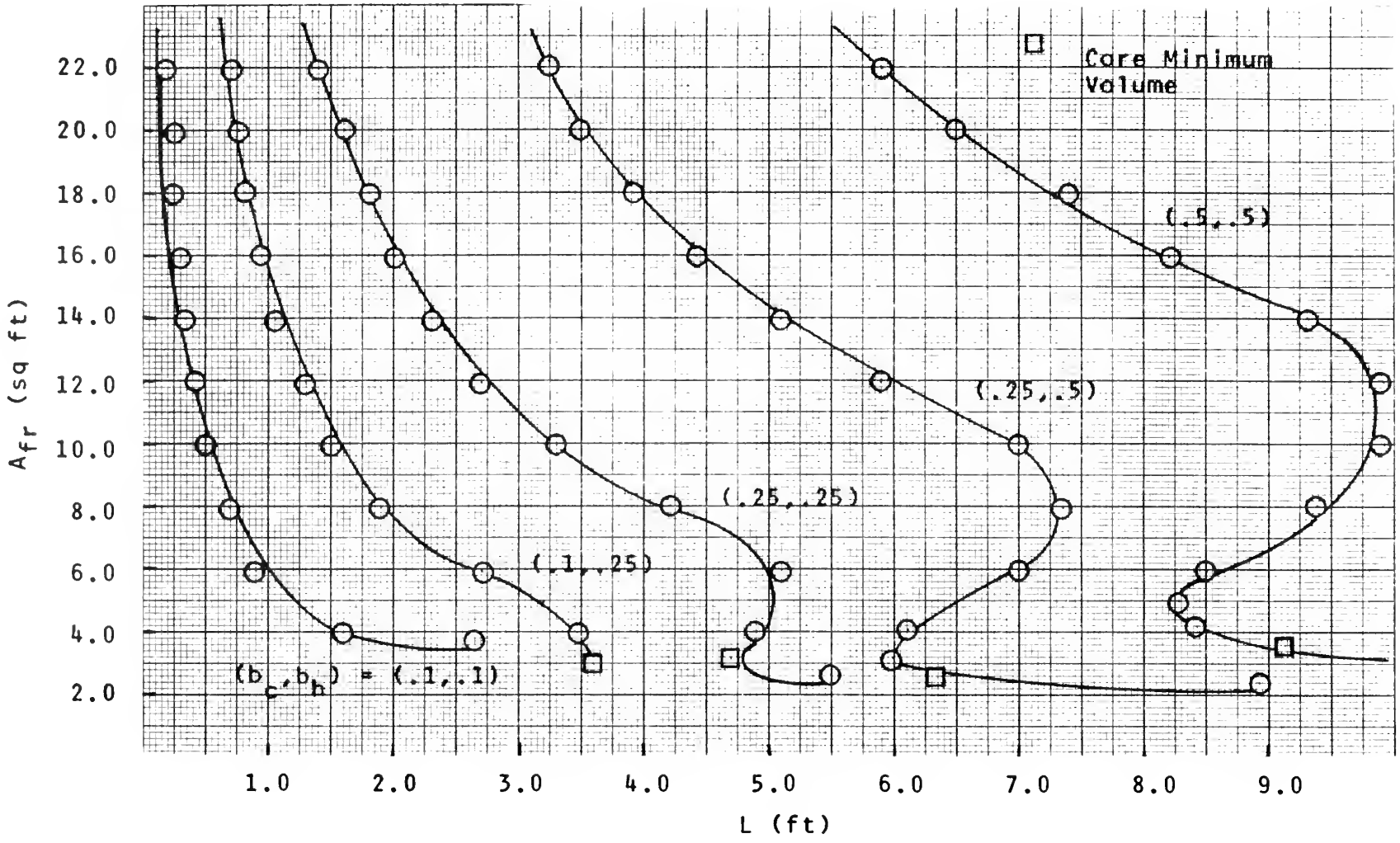

FIGURE 8 GENERAL EFFECT OF PLATE SPACINGS ON CORE DIMENSIONS

TABLE III

GENERAL RECUPERATOR PERFORMANCE AND DIMENSIONAL TRENDS

A_{fr} (sq ft)	L (ft)	V (cu ft)	Wt (lbm)	$\left(\frac{\Delta P}{P}\right)_c$	$\left(\frac{\Delta P}{P}\right)_h$	ϵ	$\dot{m}$ (lbm/hr)
b_c = 0.1 inches							
b_h = 0.1 inches							
5.0	1.31	6.55	576.4	.002	.048	.743	21393
10.0	0.51	5.10	448.8	-	.010	.703	20267
20.0	0.25	5.00	440.0	-	.002	.697	20021
30.0	0.16	4.80	422.4	-	.001	.688	20034
40.0	0.12	4.80	422.4	-	.001	.687	20022
50.0	0.10	5.00	440.0	-	-	.696	20022
b_c = 0.1 inches							
b_h = 0.5 inches							
5.0	7.01	35.05	1094.5	.050	.006	.747	21560
10.0	4.81	48.10	1502.0	.012	.001	.706	20331
20.0	2.24	44.80	1398.9	.003	-	.693	20092
30.0	1.51	45.30	1414.5	.001	-	.697	20038
40.0	1.11	44.40	1386.4	.001	-	.694	20019
50.0	0.90	45.00	1405.2	-	-	.695	20000

TABLE III
(continued)

A_{fr}	L	V	Wt	$\left(\frac{\Delta P}{P}\right)_c$	$\left(\frac{\Delta P}{P}\right)_h$	ϵ	$\dot{m}$
b_c = 0.25 inches							
b_h = 0.5 inches							
3.0	6.01	18.03	453.3	.009	.018	.718	20679
5.0	6.51	32.55	818.4	.003	.007	.701	20262
10.0	7.01	70.10	1762.5	.001	.003	.694	20083
20.0	3.51	70.20	1765.0	-	.001	.691	20034
30.0	2.34	70.20	1765.0	-	-	.690	20000
40.0	1.77	70.80	1780.1	-	-	.692	20021
50.0	1.41	70.50	1772.6	-	-	.692	20015
b_c = 0.5 inches							
b_h = 0.5 inches							
3.0	10.51	31.53	598.5	.003	.055	.748	21611
5.0	8.21	41.05	779.1	.001	.016	.706	20409
10.0	9.91	99.10	1881.0	-	.005	.696	20148
20.0	6.51	130.20	2471.2	-	.002	.691	20049
30.0	4.31	129.30	2454.2	-	.001	.690	20027
40.0	3.31	132.40	2513.0	-	-	.696	19998
50.0	2.61	130.50	2476.9	-	-	.692	20014

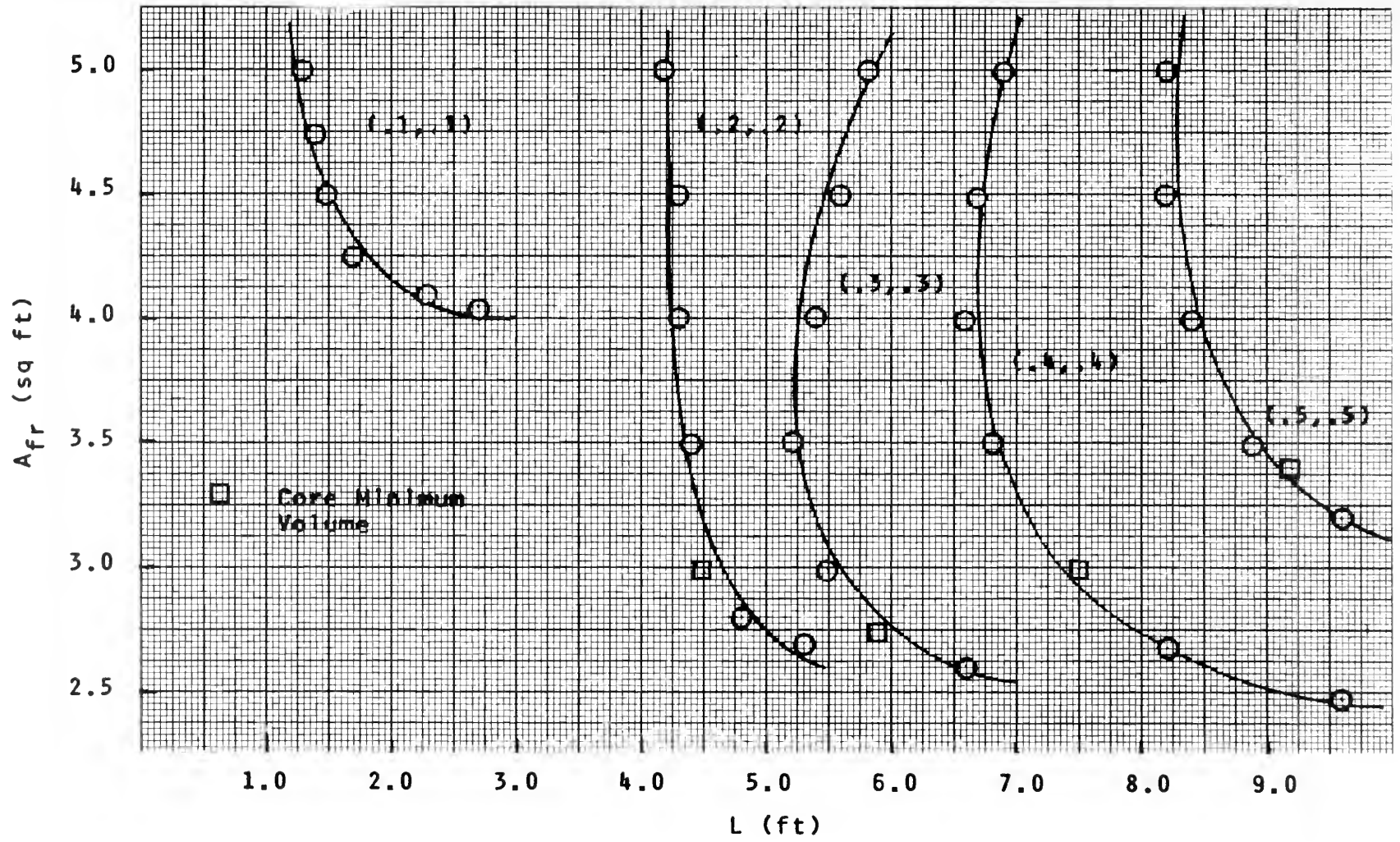

FIGURE 9 CORE DIMENSIONS FOR $b_h = b_c$

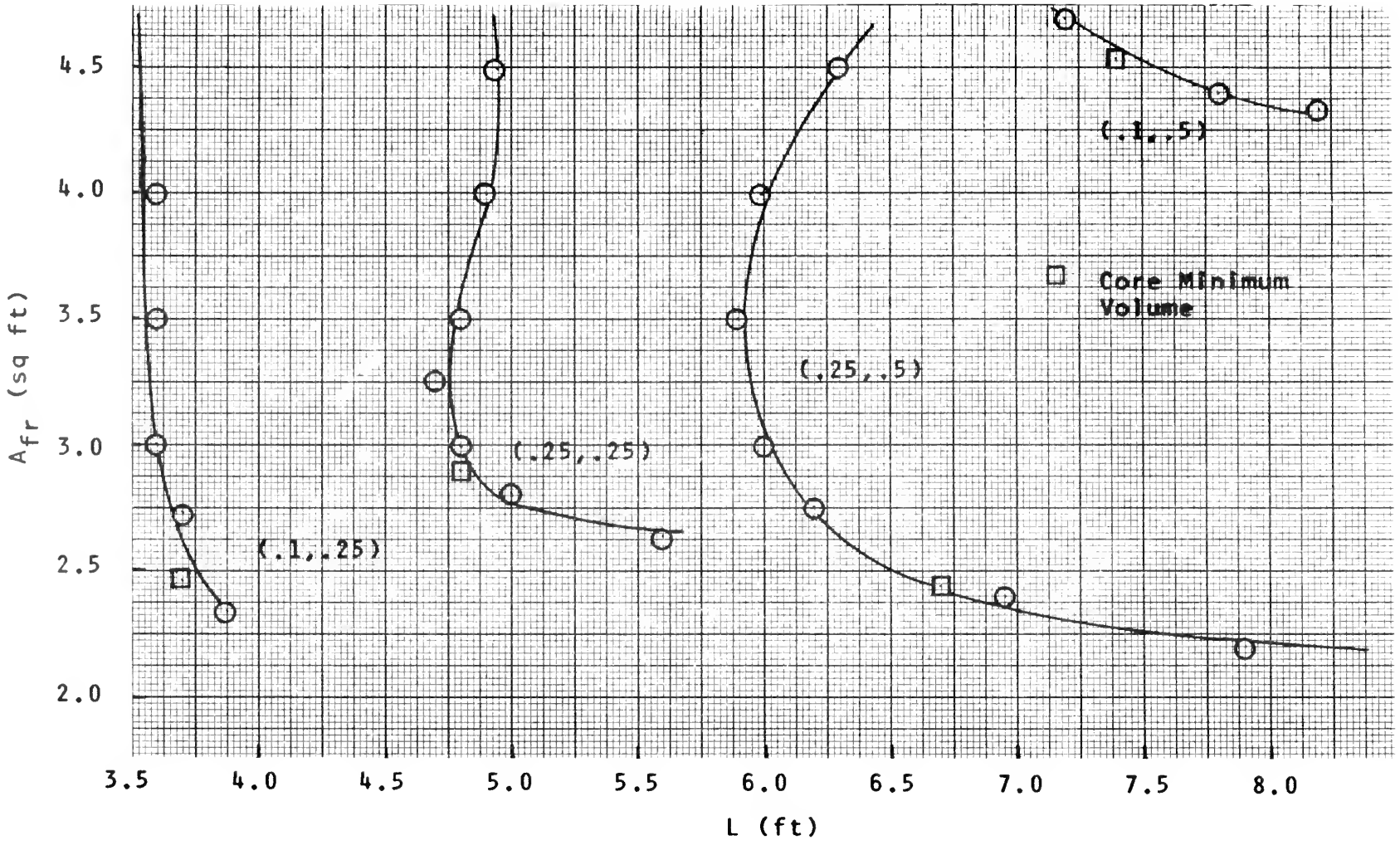

FIGURE 10 EFFECT OF UNEQUAL SPACINGS ON CORE DIMENSIONS

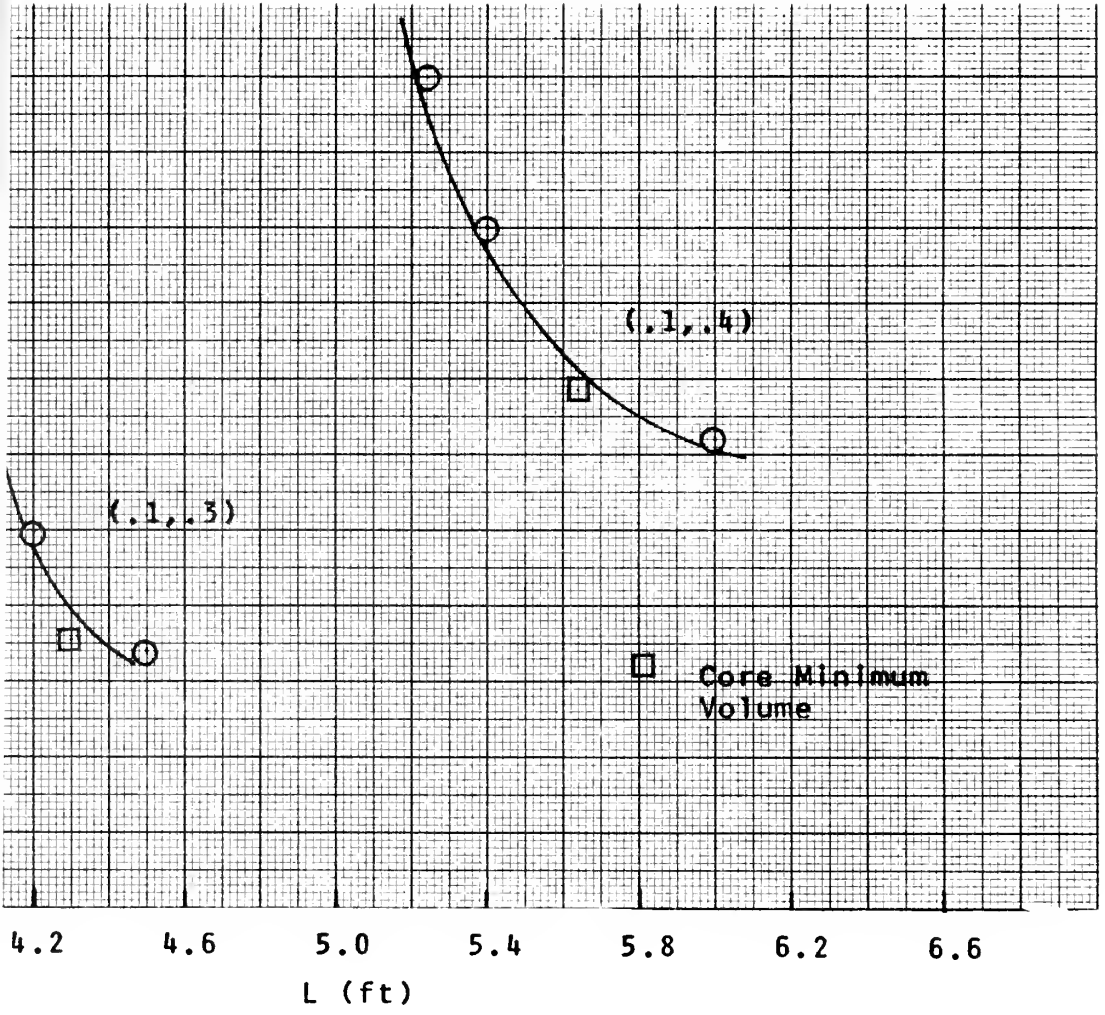

RE DIMENSIONS OF INCREASING b_h FOR b_c = 0.1 INCHES

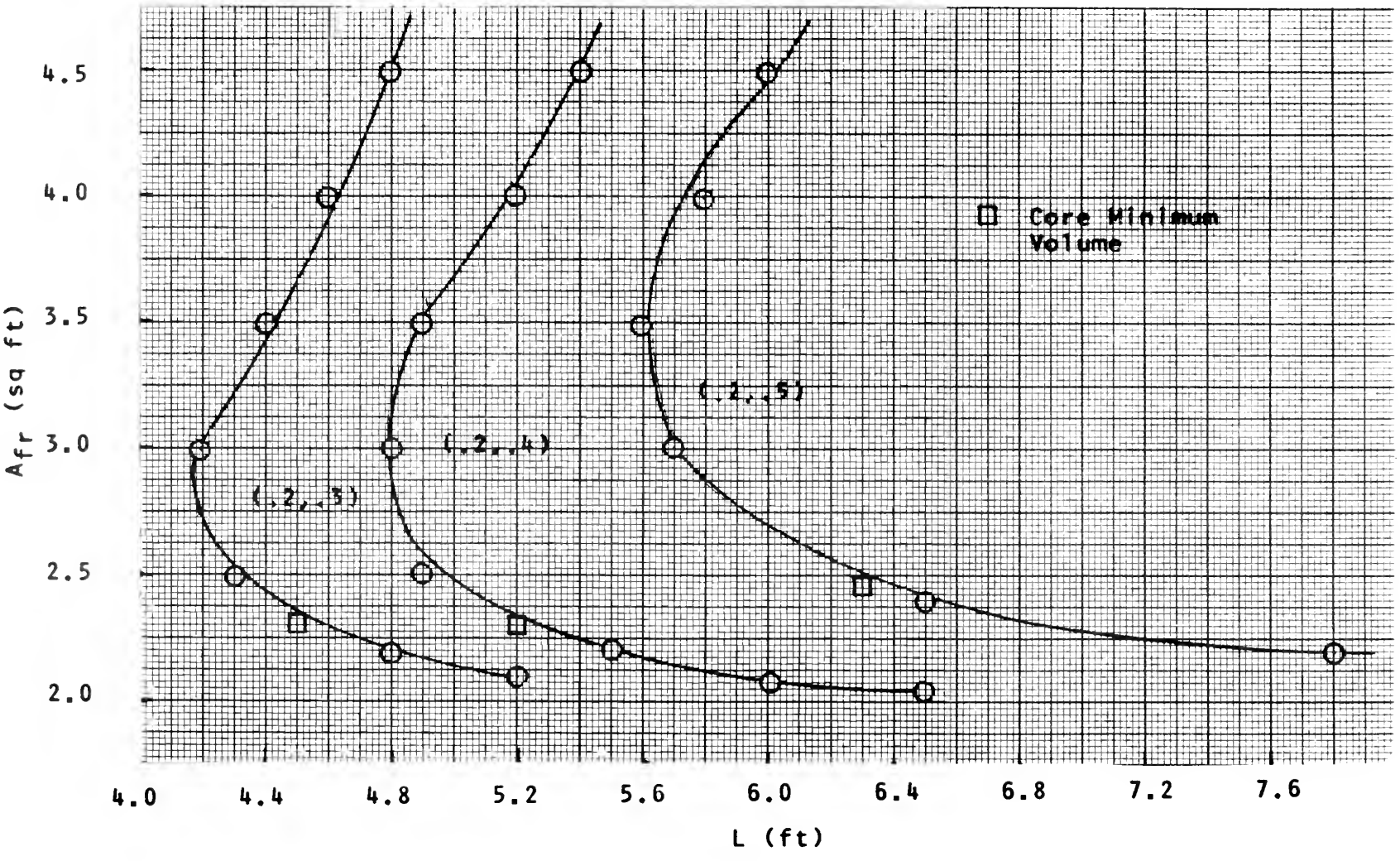

FIGURE 12 EFFECT ON CORE DIMENSIONS OF INCREASING b_h FOR b_c = 0.2 INCHES

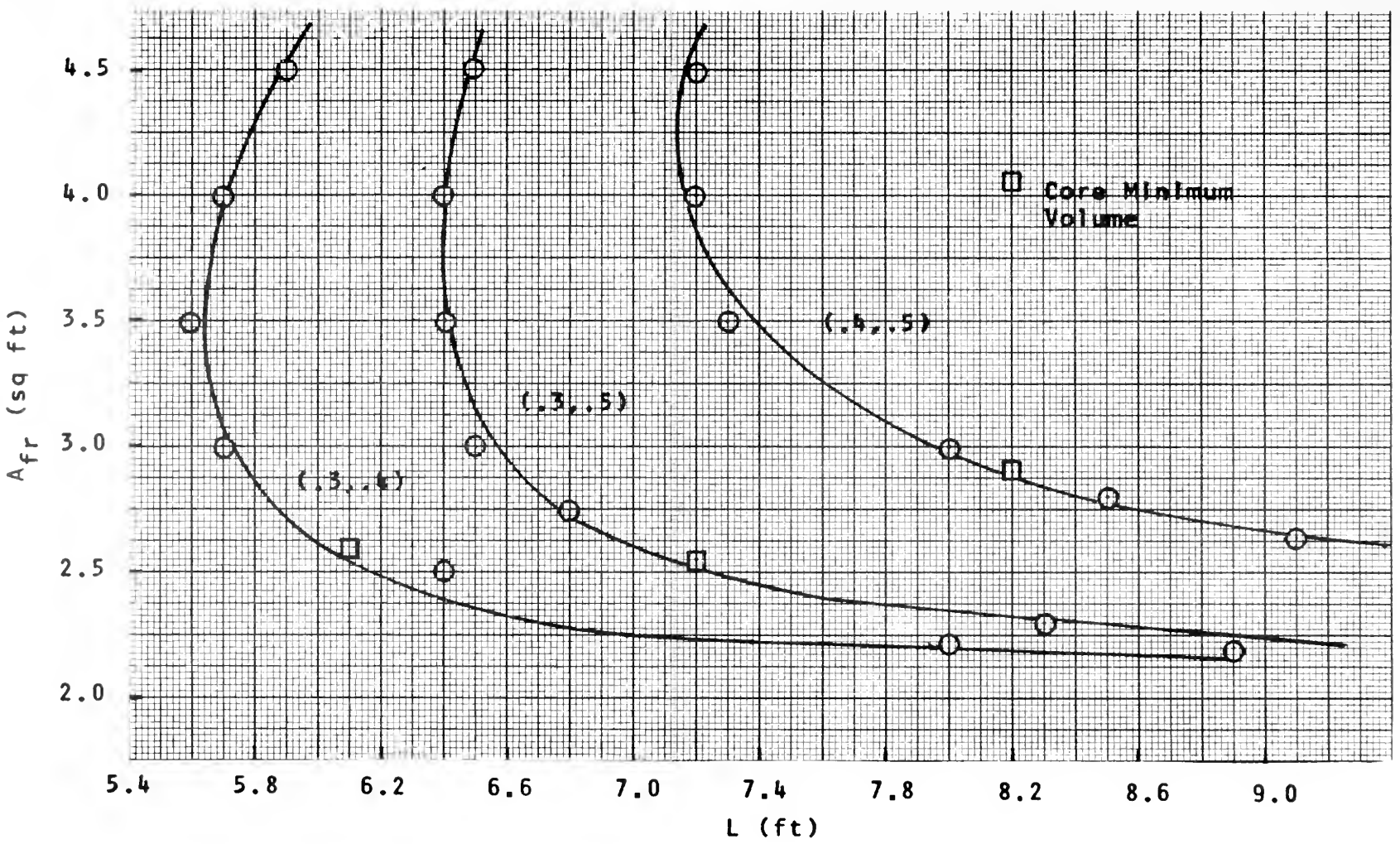

FIGURE 13 CORE DIMENSIONAL BEHAVIOR AT LARGE SPACINGS

TABLE IV

THE EFFECT ON PERFORMANCE AND DIMENSIONAL CHARACTERISTICS OF INCREASING b_h FOR CONSTANT b_c

b_h (in)	A_{fr} (sq ft)	L (ft)	V (cu ft)	Wt (lbm)	$\left(\frac{\Delta P}{P}\right)_c$	$\left(\frac{\Delta P}{P}\right)_h$	ϵ	$\dot{m}$ (lbm/hr)
b_c = 0.1 inches								
0.1	4.10	2.7	11.07	974.2	.007	.116	.816	24002
0.125	3.25	3.8	12.35	975.9	.015	.112	.817	24088
0.15	2.85	3.2	9.12	658.9	.015	.070	.775	22514
0.175	2.60	3.3	8.58	563.1	.022	.060	.771	22360
0.2	2.35	3.5	8.23	497.6	.034	.058	.781	22678
0.25	2.45	3.7	9.09	475.6	.043	.037	.768	22264
0.3	2.65	4.3	11.40	525.3	.055	.027	.772	22355
0.4	3.45	5.7	19.67	732.1	.065	.013	.768	22257
0.5	4.55	7.4	33.67	1051.4	.068	.007	.766	22186
b_c = 0.125 inches								
0.125	3.75	4.4	16.50	1183.1	.008	.122	.821	24258
0.15	3.10	3.6	11.16	732.4	.018	.079	.778	22591
0.175	2.45	3.9	9.56	578.1	.018	.092	.800	23399
0.2	2.35	3.5	8.23	461.6	.018	.065	.773	22422
0.25	2.25	3.6	8.10	397.0	.026	.047	.763	22079
0.3	2.40	3.9	9.36	407.2	.031	.032	.753	21744
0.5	3.50	6.1	21.35	640.8	.046	.010	.746	21569

TABLE IV
(continued)

b_h (in)	A_{fr} (sq ft)	L (ft)	V (cu ft)	Wt (lbm)	$\left(\frac{\Delta P}{P}\right)_c$	$\left(\frac{\Delta P}{P}\right)_h$	ϵ	$\dot{m}$ (lbm/hr)
b_c = 0.15 inches								
0.15	5.00	2.8	14.00	847.0	.002	.039	.732	21131
0.175	4.00	2.9	11.60	650.9	.008	.078	.777	22557
0.2	2.45	3.8	9.31	487.1	.012	.074	.777	22547
0.25	2.30	3.7	8.51	392.3	.016	.051	.758	21891
0.3	2.30	4.0	9.20	379.0	.021	.039	.751	21690
0.4	2.30	5.3	12.19	414.0	.042	.032	.764	22119
b_c = 0.175 inches								
0.175	3.20	4.4	14.08	736.7	.005	.082	.777	22580
0.2	2.60	4.2	10.92	535.2	.008	.084	.782	22772
0.25	2.40	3.9	9.36	407.2	.011	.055	.756	21872
0.3	2.35	4.1	9.64	376.8	.014	.042	.746	21556
0.4	2.25	5.2	11.70	380.7	.027	.035	.752	21731
b_c = 0.2 inches								
0.2	2.95	4.5	13.28	611.9	.005	.078	.774	22461
0.25	2.55	4.2	10.71	441.2	.007	.059	.758	21892
0.3	2.30	4.5	10.35	385.3	.012	.054	.756	21870
0.4	2.30	5.2	11.96	373.5	.018	.035	.743	21467
0.5	2.45	6.3	15.44	415.0	.025	.025	.740	21381

TABLE IV
(continued)

b_h (in)	A_{fr} (sq ft)	L (ft)	V (cu ft)	Wt (lbm)	$\left(\frac{\Delta P}{P}\right)_c$	$\left(\frac{\Delta P}{P}\right)_h$	ϵ	$\dot{m}$ (lbm/hr)
b_c = 0.25 inches								
0.25	2.90	4.8	13.92	518.3	.004	.064	.758	21951
0.3	2.40	5.4	12.96	440.2	.008	.073	.771	22375
0.4	2.35	5.8	13.63	393.8	.011	.043	.745	21500
0.5	2.45	6.7	16.42	412.7	.015	.029	.734	21202
b_c = 0.3 inches								
0.3	2.75	5.9	16.23	506.6	.004	.072	.767	22230
0.4	2.60	6.1	15.86	426.5	.006	.043	.739	21351
0.5	2.55	7.2	18.36	433.5	.009	.033	.732	21134
b_c = 0.4 inches								
0.4	2.95	7.5	22.13	522.4	.003	.054	.747	21575
0.5	2.90	8.2	23.78	500.4	.004	.037	.731	21106
b_c = 0.5 inches								
0.5	3.35	9.2	30.82	585.0	.002	.039	.731	21085

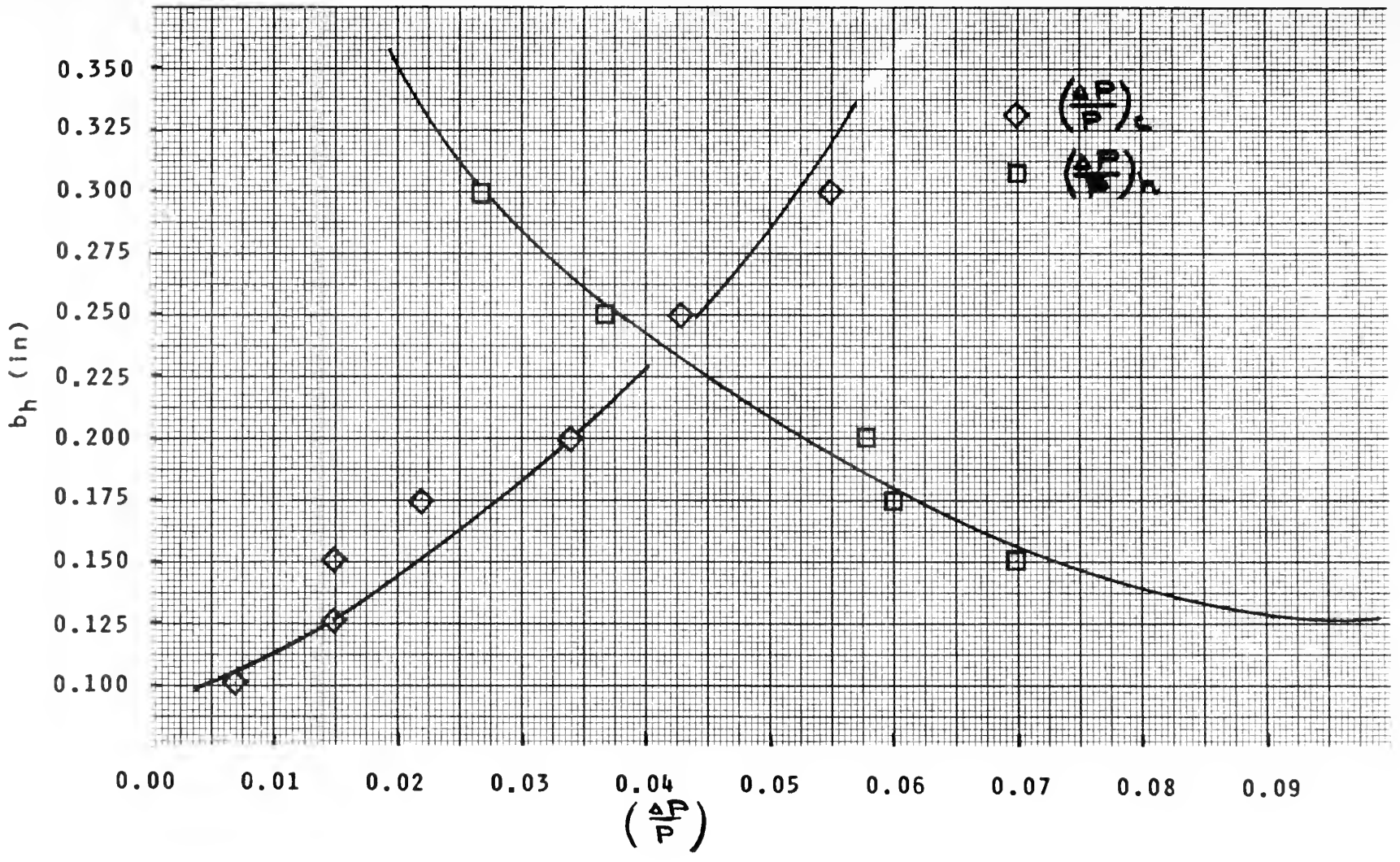

FIGURE 14 RELATIVE PRESSURE DROP AS A FUNCTION OF b_h FOR b_c = 0.1 INCHES

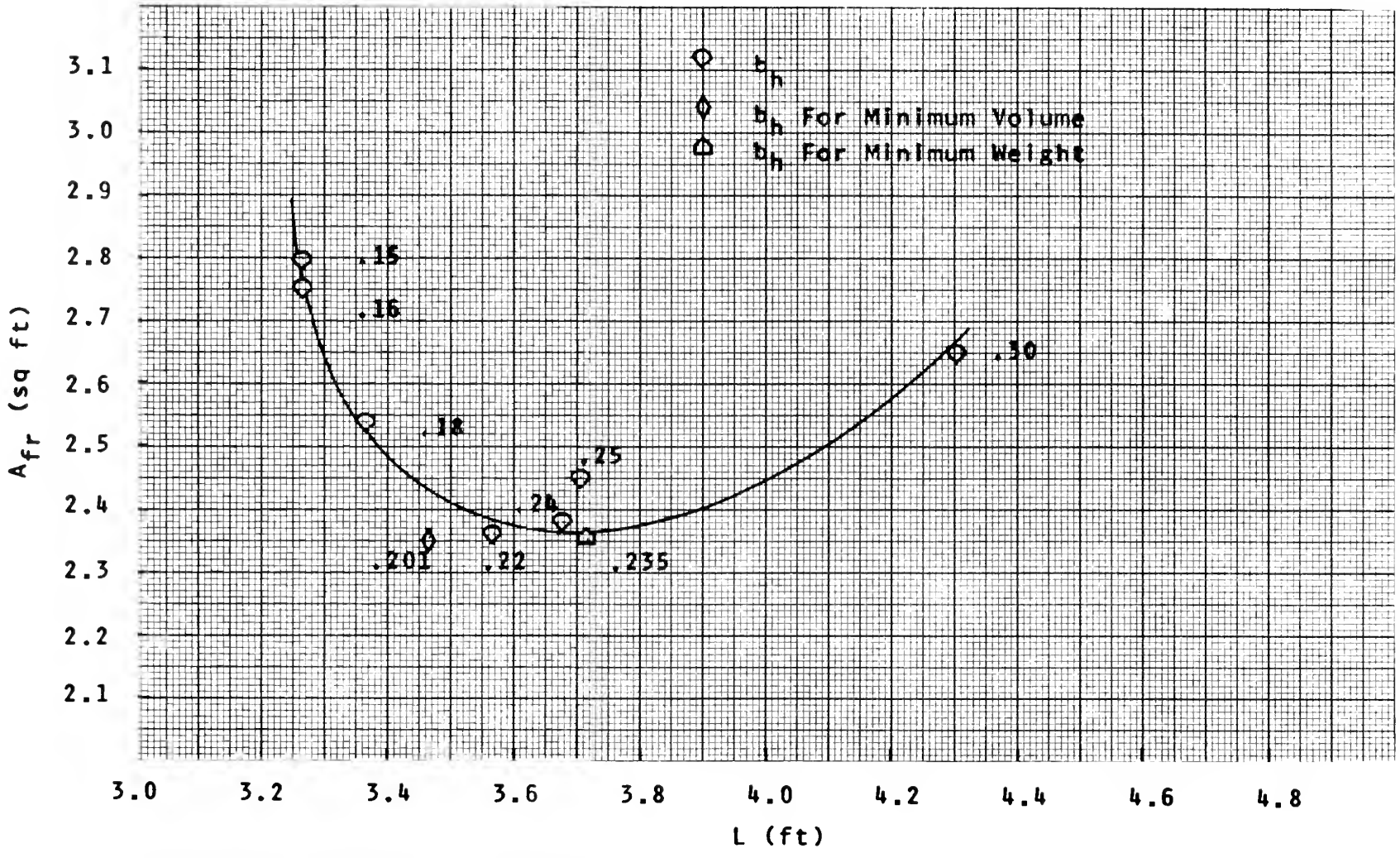

FIGURE 15 EFFECT OF INCREASING b_h ON CORE DIMENSIONS IN OPTIMUM REGION FOR b_c = 0.1 INCHES

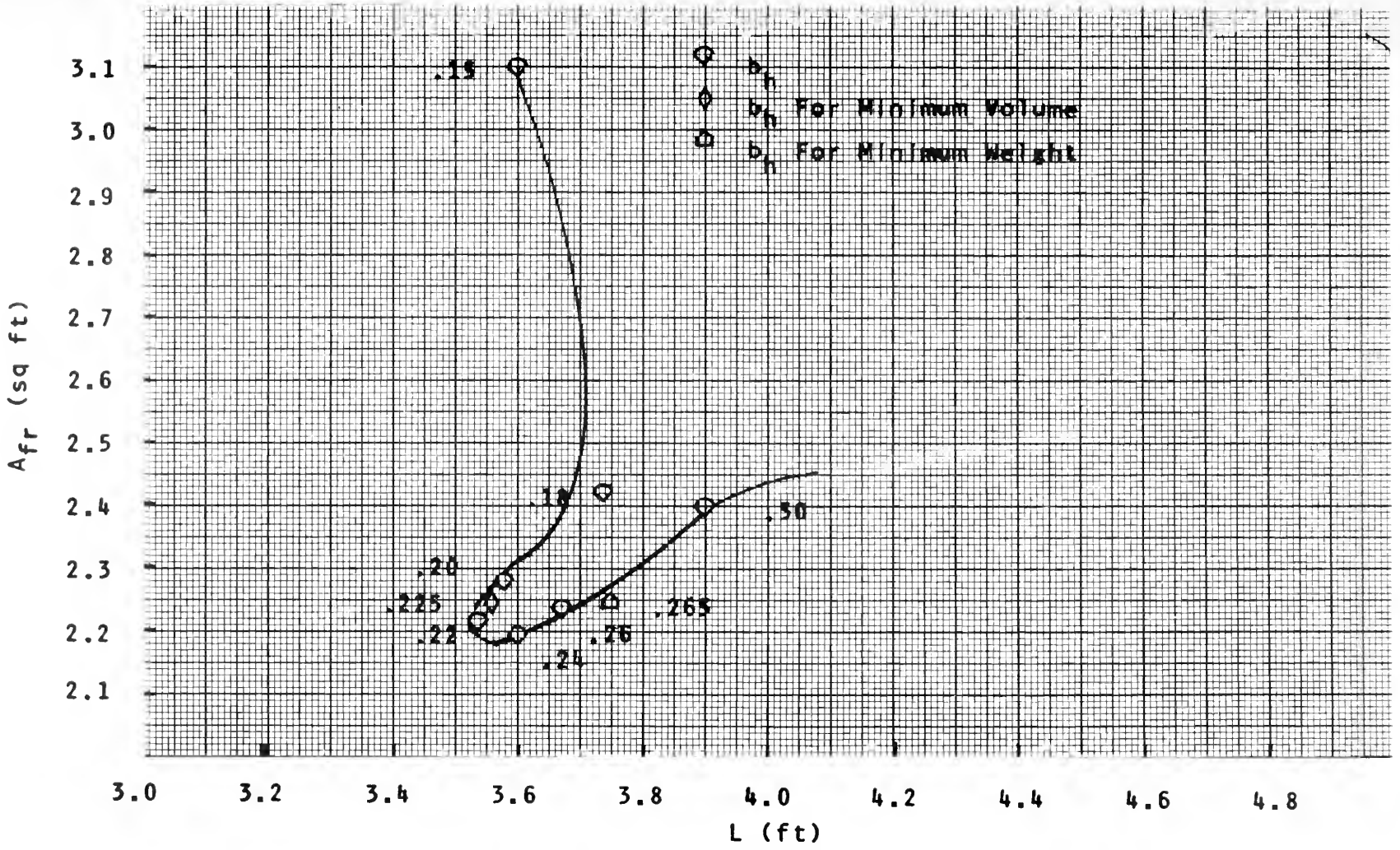

FIGURE 16 EFFECT OF INCREASING b_h ON CORE DIMENSIONS IN OPTIMUM REGION FOR b_c = 0.125 INCHES

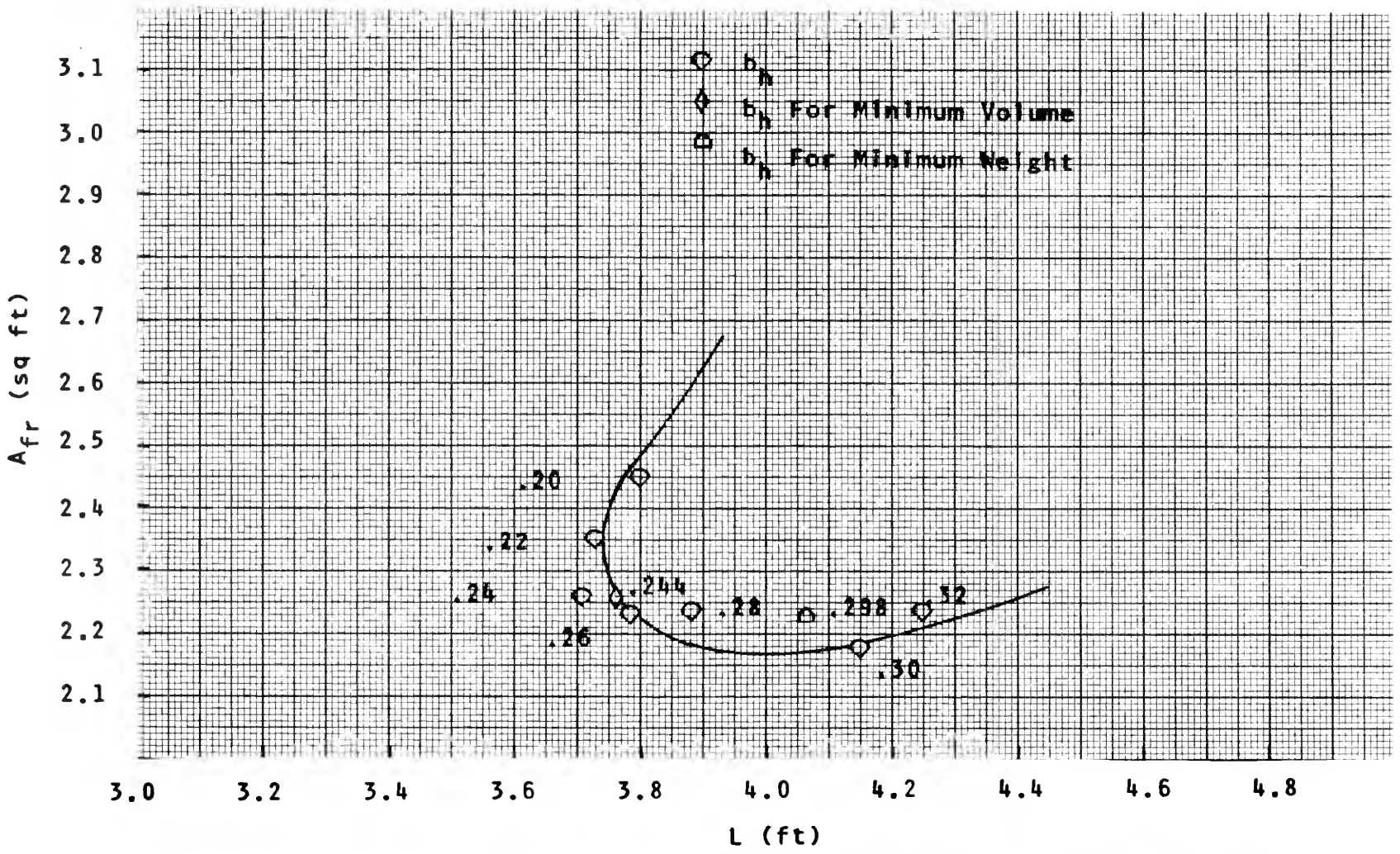

FIGURE 17 EFFECT OF INCREASING b_h ON CORE DIMENSIONS IN OPTIMUM REGION FOR b_c = 0.15 INCHES

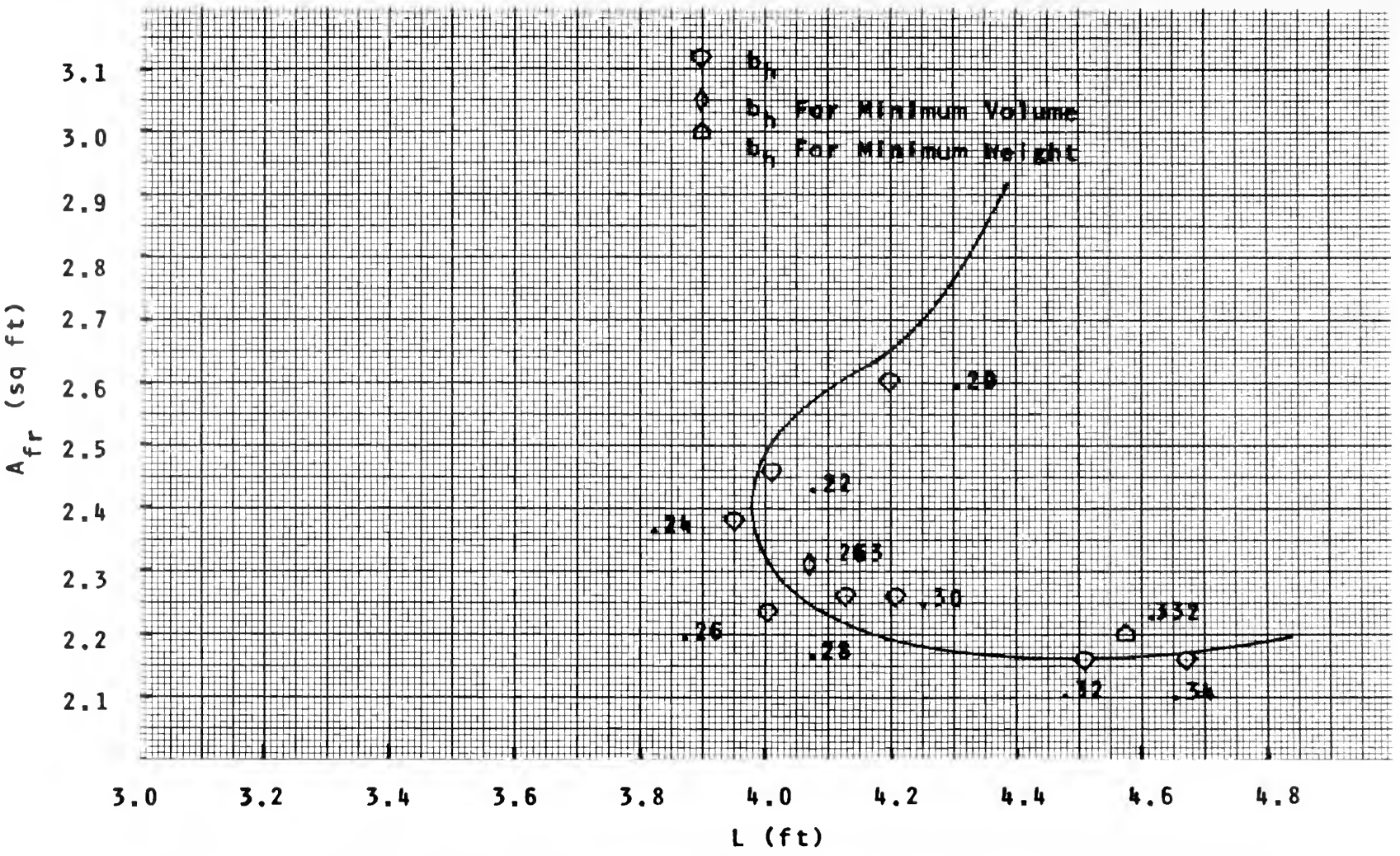

FIGURE 18 EFFECT OF INCREASING b_h ON CORE DIMENSIONS IN OPTIMUM REGION FOR b_c = 0.175 INCHES

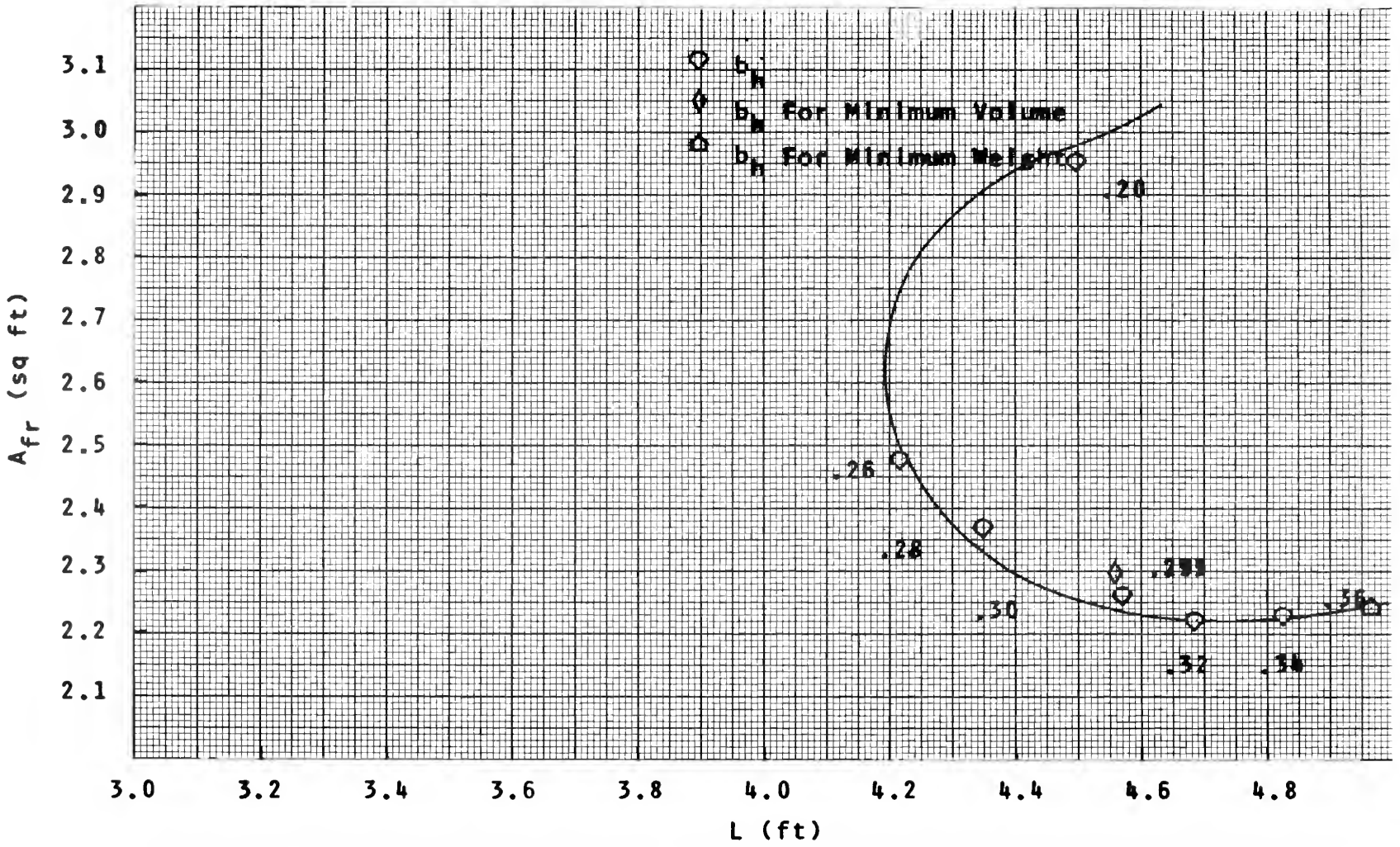

FIGURE 19 EFFECT OF INCREASING b_h ON CORE DIMENSIONS IN OPTIMUM REGION FOR b_c = 0.2 INCHES

TABLE V

CHARACTERISTICS OF MINIMUM VOLUME CORES

(b_c, b_h) (in, in)	A_{fr} (sq ft)	L (ft)	V (cu ft)	Wt (lbm)	$\left(\frac{\Delta P}{P}\right)_c$	$\left(\frac{\Delta P}{P}\right)_h$	ϵ	$\dot{m}$ (lbm/hr)
(.1,.201)	2.370	3.515	8.3305	502.43	.034	.056	.780	22645
(.125,.225)	2.240	3.560	7.9744	417.26	.024	.058	.772	22359
(.15,.244)	2.260	3.765	8.5089	397.90	.017	.057	.765	22109
(.175,.263)	2.315	4.070	9.4220	398.28	.013	.057	.761	21976
(.2,.295)	2.295	4.560	10.4652	393.41	.012	.057	.761	21965
(.25,.331)	2.386	5.378	12.8319	413.35	.009	.059	.759	21914
(.3,.351)	2.630	5.930	15.5959	449.98	.005	.055	.752	21686

TABLE VI

CHARACTERISTICS OF MINIMUM WEIGHT CORES

(b_c, b_h) (in, in)	A_{fr} (sq ft)	L (ft)	V (cu ft)	Wt (lbm)	$\left(\frac{\Delta P}{P}\right)_c$	$\left(\frac{\Delta P}{P}\right)_h$	ϵ	$\dot{m}$ (lbm/hr)
(.1,.235)	2.365	3.710	8.7741	478.50	.043	.045	.778	22564
(.125,.265)	2.250	3.745	8.4261	397.88	.030	.044	.764	22106
(.15,.298)	2.230	4.065	9.1430	378.22	.024	.044	.759	21900
(.175,.332)	2.200	4.575	10.0650	369.75	.020	.045	.757	21849
(.2,.36)	2.240	4.965	11.1216	371.23	.016	.043	.751	21651
(.25,.392)	2.405	5.625	13.5281	395.63	.010	.042	.743	21417
(.3,.428)	2.575	6.445	16.5959	429.54	.007	.040	.738	21278

TABLE VII

CHARACTERISTICS OF $b_h = 2b_c$ CORES

(b_c, b_h) (in, in)	A_{fr} (sq ft)	L (ft)	V (cu ft)	Wt (lbm)	$\left(\frac{\Delta P}{P}\right)_c$	$\left(\frac{\Delta P}{P}\right)_h$	ϵ	$\dot{m}$ (lbm/hr)
(.1,.2)	2.370	3.515	8.3305	504.00	.033	.057	.781	22660
(.125,.25)	2.230	3.660	8.1618	400.03	.028	.049	.767	22180
(.15,.3)	2.210	4.155	9.1825	378.24	.025	.045	.761	21974
(.175,.35)	2.170	4.820	10.4594	271.55	.024	.044	.759	21923
(.2,.4)	2.280	5.295	12.0726	376.98	.019	.036	.746	21501
(.25,.5)	2.450	6.800	16.6600	418.88	.015	.030	.736	21224

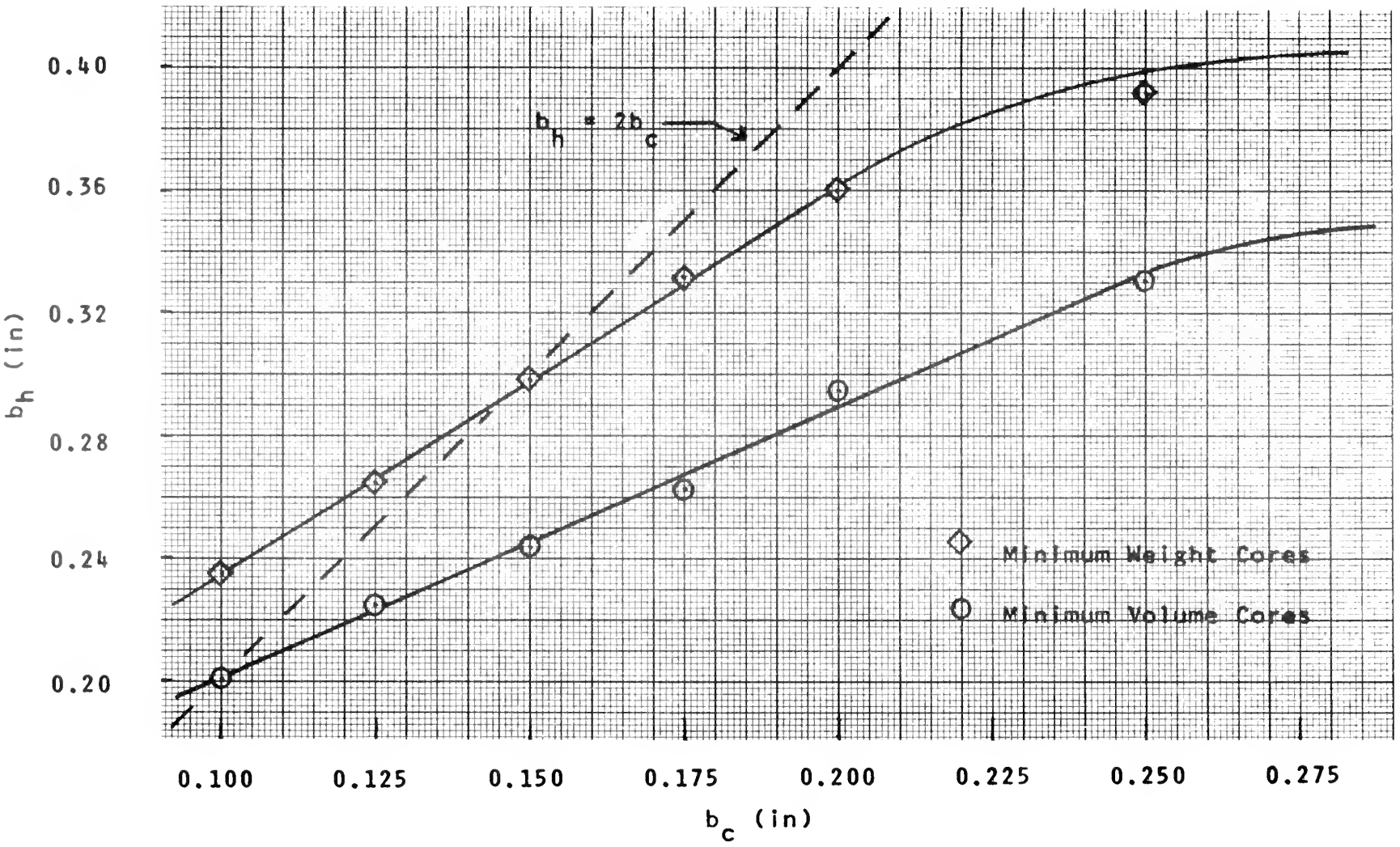

FIGURE 20 OPTIMUM RECUPERATOR CORE SPACINGS WITH RESPECT TO WEIGHT AND VOLUME

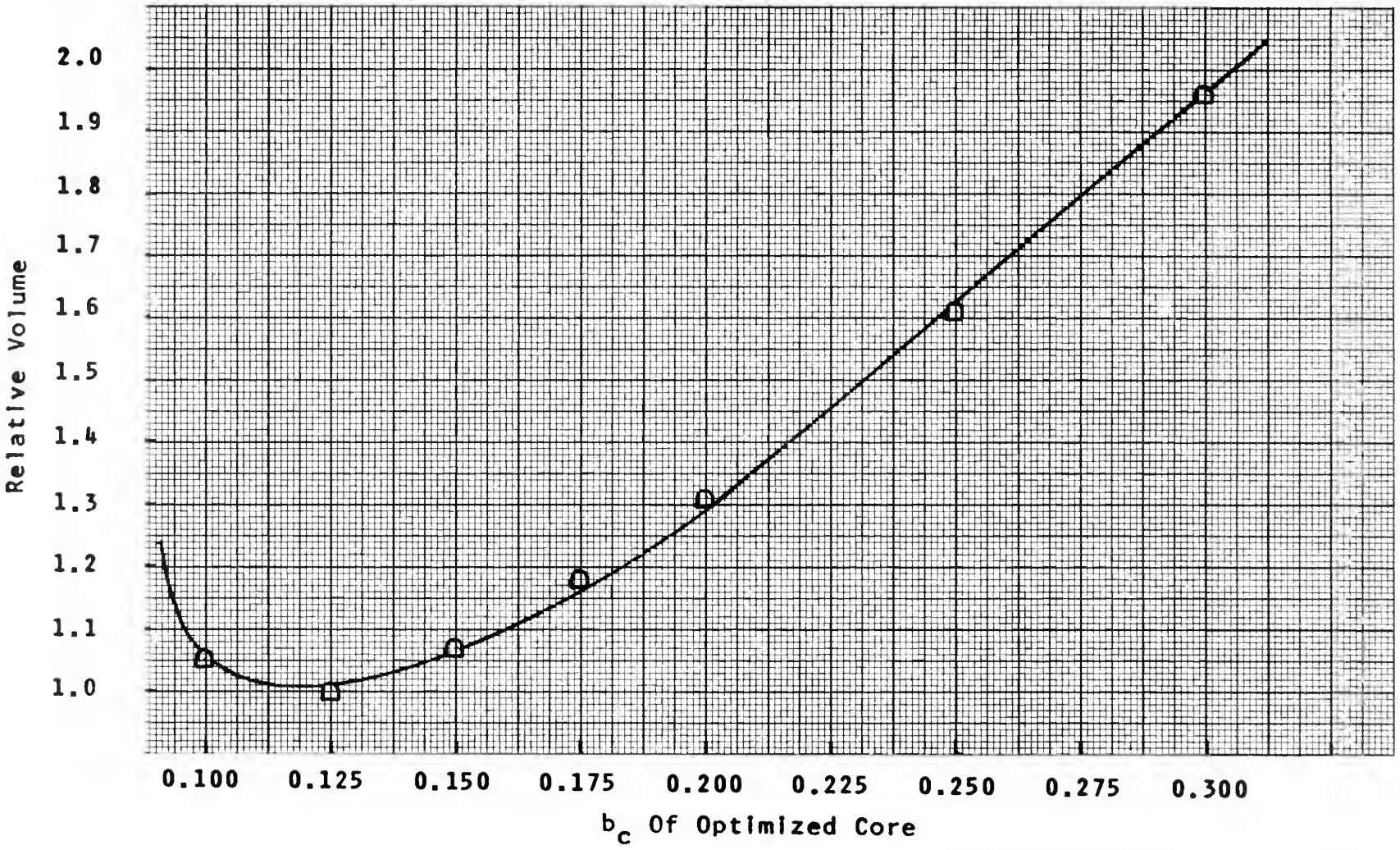

FIGURE 21 RELATIVE VOLUMES OF OPTIMIZED CORES WITH RESPECT TO THE MINIMUM VOLUME CORE

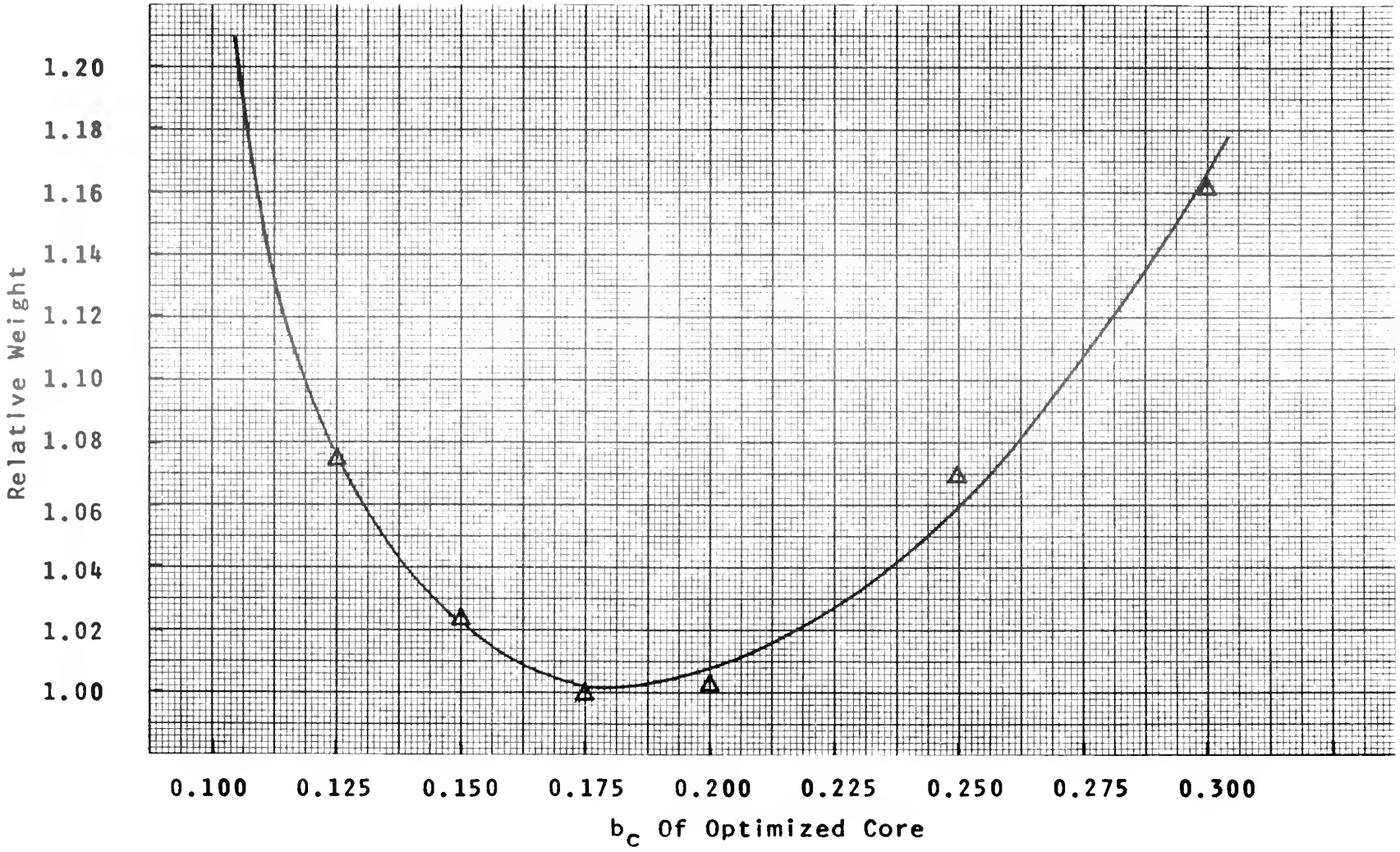

FIGURE 22 RELATIVE WEIGHTS OF OPTIMIZED CORES WITH RESPECT TO THE MINIMUM WEIGHT CORE

APPENDIX A

THE REGENERATED BRAYTON CYCLE

A. THERMODYNAMICS

Ideally, the basic open cycle consists of the four processes of isentropic compression, constant pressure heat addition, isentropic expansion, and constant pressure heat rejection [4]. The ideal regenerated cycle differs only in that the heat addition process is accomplished through the use of a recuperator as well as the standard combustor. With these points in mind, the ideal cycle (refer to Figure 23) may be described using the equalities:

$$P_{2a} = P_{3a} = P_{4a} \qquad \text{A.1}$$

$$P_{5a} = P_{6a} \qquad \text{A.2}$$

$$T_{2a} = T_{6a} \qquad \text{A.3}$$

$$T_{3a} = T_{5a} \qquad \text{A.4}$$

The most obvious differences between the actual and ideal cycles, from the thermodynamic viewpoint, are the increases of entropy and drops in pressure due to actual working conditions. These differences may be best explained by taking the cycle in its respective stages.

1. Compression

State point "2" lies to the right, at an increased entropy, of ideal point "2a" due to the irreversibility of the compression process; both points, however, lie on a line of constant pressure, since the compressor outlet pressure is specified by working conditions. The resulting equality is

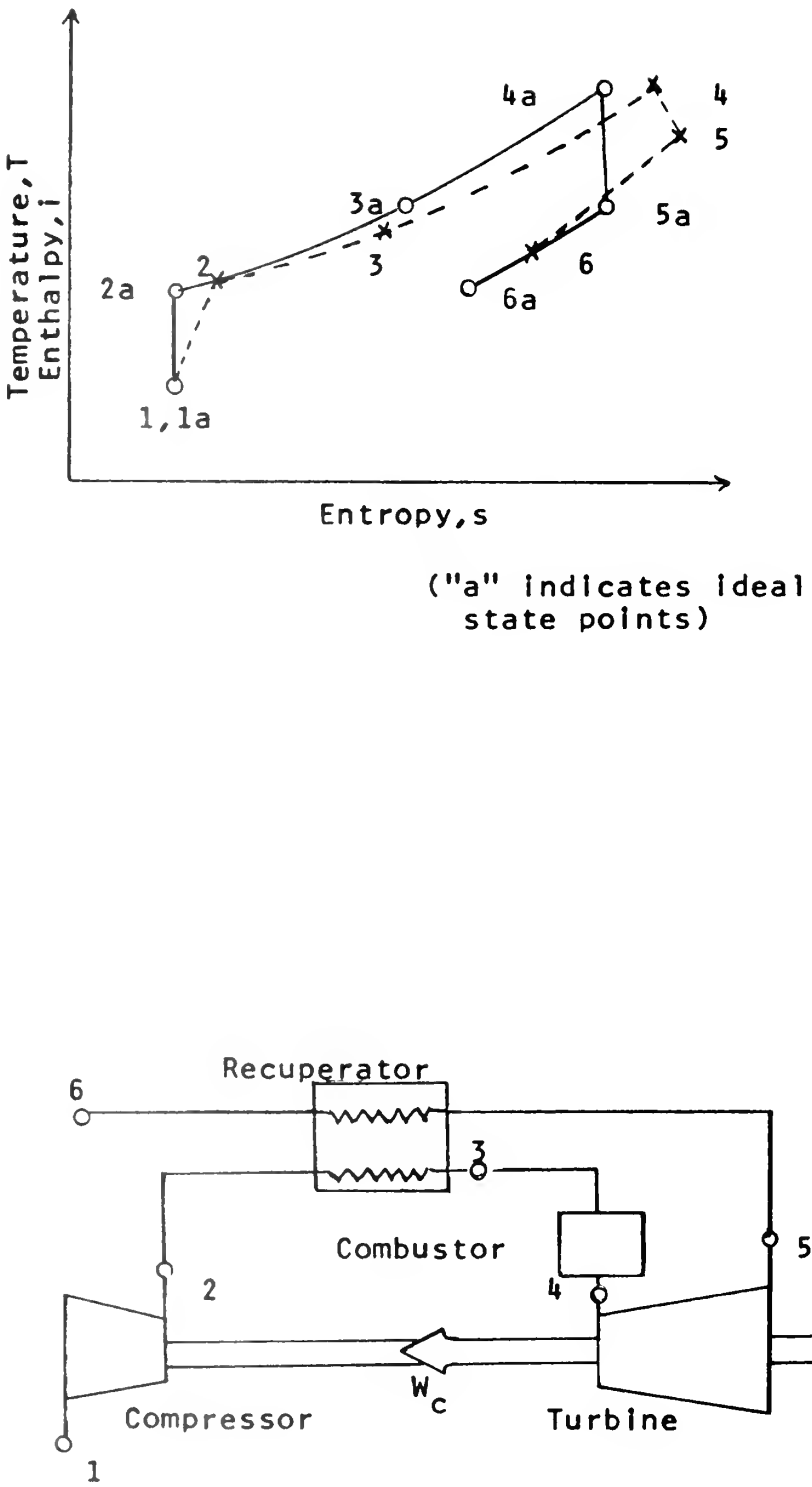

FIGURE 23 THE ACTUAL AND IDEAL REGENERATED BRAYTON CYCLES

$$P_{2a} = P_2 \qquad \text{A.5}$$

2. Heat Addition

Two changes are apparent when one compares cycle conditions at the recuperator exit point. First, the actual pressure level is below that of the ideal, due to the pressure drop as the air flows through the recuperator.

$$P_3 < P_{3a} \qquad \text{A.6}$$

Second, the temperature of the actual case is below that for the ideal, since less heat is transferred than for the reversible process.

$$T_3 < T_{3a} \qquad \text{A.7}$$

In order to raise the temperature further, the air flows through a combustor. The inlet temperature of the turbine is specified by its material properties,

$$T_{4a} = T_4 \qquad \text{A.8}$$

However, point "4" does lie at an entropy state greater than point "4a" due to the irreversibilities involved between the compressor and the turbine. Furthermore, an additional pressure drop occurs as the air flows through the combustor.

$$P_4 < P_{4a} \qquad \text{A.9}$$

3. Expansion

An additional entropy increase results from the expansion process in the turbine, moving point "5" to the right of the ideal state point. As the turbine outlet pressure is not specified, and a further pressure drop is expected as the gases pass through the recuperator,

the pressure at point "5" is necessarily greater than that for the ideal cycle.

$$P_5 > P_{5a} \qquad \text{A.10}$$

4. Heat Rejection

As indicated, the pressure drop experienced by the hot gases in passing through the recuperator results in the pressure at point "6" being equal to the ideal pressure, since this point is considered to be the exhaust to atmospheric conditions.

$$P_{6a} = P_6 = 14.696 \text{ psi} \qquad \text{A.11}$$

Finally, since less heat is transferred from the hot gases to the incoming cold air as is ideally possible, the temperature at point "6" is greater than that for the ideal case.

$$T_6 > T_{6a} \qquad \text{A.12}$$

B. CYCLE SYSTEMS

An understanding of the efficiencies of each system is necessary if one is to work with the Brayton cycle. This may best be accomplished by looking at each system process individually. It must be noted that the assumption of steady flow and no potential energy change of position is made for the cycle. More detailed information may be obtained in Refs. [3] and [5].

1. Compressor

η_c = compressor efficiency

$$\eta_c = \frac{\text{work of isentropic compression}}{\text{actual internal work}} = \frac{i_{1a} - i_{2a}}{i_1 - i_2} \qquad \text{A.13}$$

2. Recuperator

ϵ = recuperator effectiveness

$$\epsilon = \frac{\text{actual heat transfer}}{\text{maximum possible heat transfer}}$$

$$\epsilon = \frac{(\dot{m}c_p)_h (T_{h,in} - T_{h,out})}{(\dot{m}c_p)_{min} (T_{h,in} - T_{c,in})} = \frac{(\dot{m}c_p)_c (T_{c,out} - T_{c,in})}{(\dot{m}c_p)_{min} (T_{h,in} - T_{c,in})} \quad \text{A.14}$$

A more detailed explanation of recuperator effectiveness is presented in Section IV.

3. Combustor

η_{COMB} = combustor efficiency

$$\eta_{COMB} = \frac{\text{actual energy received by gases}}{\text{energy released during complete combustion}}$$

$$\eta_{COMB} = \frac{(1 + r_{f/a}) i_4 - i_3 - r_{f/a} i_f}{r_{f/a} q_l} \quad \text{A.15}$$

This definition may be more easily understood when an energy balance based on one pound of air and $r_{f/a}$ pounds of fuel per pound of air entering the combustor is made.

$$r_{f/a} i_f + r_{f/a} q_l + i_3 = (1 + r_{f/a}) i_4 + (1 - \eta_{COMB}) r_{f/a} q_l \quad \text{A.16}$$

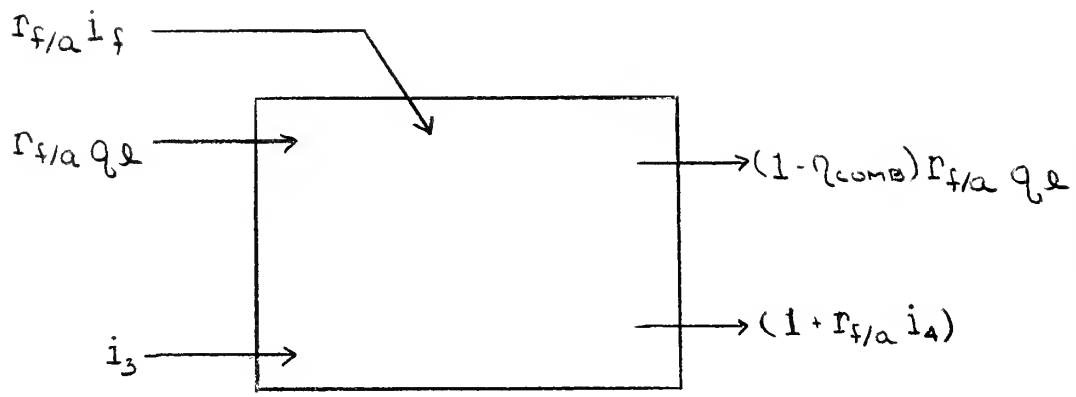

FIGURE 24

COMBUSTOR ENERGY DIAGRAM

of the three entering energy terms, it can readily be seen that i_3 (the enthalpy of the incoming air) and $r_{f/a} i_f$ (the fuel to air ratio times the enthalpy of the fuel) represent molecular internal energy and flow work. The third term represents the chemical energy stored in the fuel, $r_{f/a} q_1$; since complete condensation of water vapor in the air flow will not occur, the lower heating value of the fuel (which disregards the latent heat of condensation), q_1, is usually used in gas turbine analysis [3].

The fuel to air ratio, a very important parameter in the gas turbine analysis, may now be shown to be

A.17

4. Turbine

η_t = turbine efficiency

$$\eta_t = \frac{\text{actual internal work}}{\text{work of isentropic expansion}}$$

$$\eta_t = \frac{i_4 - i_5}{i_{4a} - i_{5a}} \qquad \text{A.18}$$

5. Additional Calculations

Three final calculations are frequently useful in a complete analysis.

Overall Thermal Efficiency

η_{th} = overall thermal efficiency

$$\eta_{th} = \frac{\text{net work}}{\text{heat supplied}}$$

$$\eta_{th} = \frac{(1+r_{f/a})(i_4 - i_3) - (i_2 - i_1)}{r_{f/a}\, q_1} \qquad \text{A.19}$$

Horsepower

Using the conversion factor 2544 BTU = one horsepower-hour, the equation for the horsepower output may be seen to be

$$HP = \frac{(\eta_{th})(r_{f/a})(q_1)(\dot{m}_2)}{2544} \qquad \text{A.20}$$

Specific Fuel Consumption

$$SFC = \frac{\text{fuel burned}}{\text{net work}}$$

$$SFC = \frac{(r_{f/a})(\dot{m})}{HP} \qquad \text{A.21}$$

$$SFC = \frac{2544}{q_1} \qquad \text{A.22}$$

APPENDIX B

COMPUTER PROGRAM ESSENTIAL FEATURES

A. GENERAL ASPECTS

The computer program referred to in Ref. [1] has been greatly expanded by Professor P. F. Pucci since its original use, and may now be used to investigate parallel and crossflow, as well as counterflow, recuperator characteristics. This counterflow analysis is based on design parameters for the Orenda OT-4 gas turbine only; the program, however, is applicable to any gas turbine recuperator analysis, as the desired design points are introduced as input data. A basic understanding of the program logic may be obtained by referring to the simplified flow chart, Figure 25; a sample program output is presented in Figure 28.

The program is written on the basis that changes in recuperator core geometry (plate spacings and fin configurations) and dimensions (frontal area and length) are reflected directly in the overall cycle thermal efficiency, rather than in the often used design variables of heat exchanger pressure drop and heat transfer characteristics. Although the program may be used to obtain data for a number of conditions (such as the computation of: (1) the maximum cycle thermal efficiency given a recuperator of specified volume, (2) recuperator dimensions necessary to obtain a specified thermal efficiency and, (3) general outputs for a simple open cycle, to mention only a few) only two output types were used extensively in the analysis.

The first, Output Type III, computes the required recuperator length for a specified frontal area and internal geometry; furthermore, the horsepower and cycle thermal efficiency are specified, within predetermined tolerance levels. This output is extremely useful in providing an overall picture of the desired recuperator's behavior over a wide range of frontal areas. Information on the effect of changes in internal core dimensions, may be obtained with the use of Output Type VIII. This routine, similar to Output Type III, computes the required length of a recuperator over a range of frontal areas. In this procedure, however, the cold side plate spacing remains constant, as before, whereas the hot side plate spacing is incremented over a desired range. Flow charts for these routines are presented in Figures 26 and 27.

B. PARAMETRIC APPROXIMATIONS

As explained in Section IV, the computer program makes use of polynomial approximations to obtain a number of fundamental parameters. The polynomial coefficients used in this analysis will be presented, should a need for them arise in the future; unless otherwise indicated, the polynomial is of the form

$$P(x) = A_1 + A_2x + A_3x^2 + \ldots\ldots\ldots\ldots + A_ix^{i-1} \qquad \text{B.1}$$

where: $P(x)$ = desired parameter

x = variable on which the parameter is based

A_i = polynomial coefficients

$i-1$ = order of polynomial

Fanning Friction Factor (function of Re; $1000 < Re < 5000$)

$A_1 = -1.311518618929068 \times 10^{-1}$ $A_7 = -1.590750036125343 \times 10^{-19}$

$A_2 = 7.522772995845896 \times 10^{-4}$ $A_8 = 3.138452606608756 \times 10^{-23}$

$A_3 = -1.550552244236629 \times 10^{-6}$ $A_9 = -3.933692644883426 \times 10^{-27}$

$A_4 = 1.730155685156651 \times 10^{-9}$ $A_{10} = 2.838094432805311 \times 10^{-31}$

$A_5 = -1.189041200805969 \times 10^{-12}$ $A_{11} = -8.976537263266828 \times 10^{-36}$

$A_6 = 5.329916594794135 \times 10^{-16}$

Colburn-j Factor (function of Re; $1000 < Re < 5000$)

$A_1 = 1.644630125351775 \times 10^{-1}$ $A_7 = 1.100442463486636 \times 10^{-19}$

$A_2 = -6.796500408006909 \times 10^{-4}$ $A_8 = -2.152007282686803 \times 10^{-23}$

$A_3 = 1.238993655152145 \times 10^{-6}$ $A_9 = 2.683333339022575 \times 10^{-27}$

$A_4 = -1.292429783097030 \times 10^{-9}$ $A_{10} = -1.930653368061576 \times 10^{-31}$

$A_5 = 8.543160388163581 \times 10^{-13}$ $A_{11} = 6.099637443396928 \times 10^{-36}$

$A_6 = -3.740734237674230 \times 10^{-16}$

Prandtl Number (function of temperature)

$A_1 = 0.7865630968$ $A_6 = -0.1973361281 \times 10^{-14}$

$A_2 = -0.2871584338 \times 10^{-4}$ $A_7 = 0.1041204710 \times 10^{-17}$

$A_3 = 0.3666074673 \times 10^{-6}$ $A_8 = -0.2047252924 \times 10^{-21}$

$A_4 = -0.1373281188 \times 10^{-9}$ $A_9 = -0.1538501631 \times 10^{-25}$

$A_5 = 0.1569904076 \times 10^{-11}$ $A_{10} = 0.7960530427 \times 10^{-29}$

Viscosity (function of temperature)

$$\mu = \frac{(Q) \times (1.716 \times 10^{-10}) \times 3600.0}{14.822} \qquad \text{B.2}$$

where Q is determined by the polynomial equation (as a function of temperature) of coefficients:

$A_1 = -0.4132588012 \times 10^{-1}$ $A_6 = -0.5752187450 \times 10^{-15}$

$A_2 = 0.2706898585 \times 10^{-2}$ $A_7 = 0.2117993215 \times 10^{-18}$

$A_3 = -0.1318733093 \times 10^{-5}$ $A_8 = -0.3862860359 \times 10^{-22}$

$A_4 = 0.7538864121 \times 10^{-12}$ $A_9 = 0.2782105119 \times 10^{-26}$

$A_5 = 0.7221455415 \times 10^{-12}$ $A_{10} = 0.6763288488 \times 10^{-32}$

Specific Heat (function of temperature)

$A_1 = 0.24913875 \times 10^{0}$ $A_4 = -0.21358038 \times 10^{-10}$

$A_2 = -0.48196782 \times 10^{-4}$ $A_5 = 0.48224330 \times 10^{-15}$

$A_3 = 0.68100588 \times 10^{-7}$ $A_6 = 0.47985777 \times 10^{-18}$

Enthalpy (function of temperature)

$A_1 = -0.97746770 \times 10^{2}$ $A_4 = 0.30219636 \times 10^{-7}$

$A_2 = 0.25257199 \times 10^{0}$ $A_5 = -0.94272843 \times 10^{-11}$

$A_3 = -0.31167200 \times 10^{-4}$ $A_6 = 0.11868992 \times 10^{-14}$

$A_7 = -0.32615268 \times 10^{-19}$

Relative Pressure (function of temperature)

$$P_{rel} = 0.1 \exp(D) \qquad \text{B.3}$$

where D is determined by the polynomial equation (as a function of temperature) of coefficients:

$A_1 = -0.4043080 \times 10^{1}$ $A_6 = 0.21127191 \times 10^{-13}$

$A_2 = 0.2759446 \times 10^{-1}$ $A_7 = -0.67216409 \times 10^{-17}$

$A_3 = -0.45085958 \times 10^{-4}$ $A_8 = 0.12101712 \times 10^{-20}$

$A_4 = 0.53019327 \times 10^{-7}$ $A_9 = -0.94003173 \times 10^{-25}$

$A_5 = -0.41468032 \times 10^{-10}$

Temperature (function of enthalpy)

The temperature is computed in the standard polynomial form, as a function of x, where

$$x = \log(10.0 \cdot \text{temperature}) \qquad \text{B.4}$$

$A_1 = 0.23796617 \times 10^{3}$ $\quad$ $A_6 = -0.45916847 \times 10^{0}$

$A_2 = 0.37807000 \times 10^{1}$ $\quad$ $A_7 = 0.33772184 \times 10^{-1}$

$A_3 = 0.49211414 \times 10^{2}$ $\quad$ $A_8 = -0.13466334 \times 10^{-2}$

$A_4 = -0.15095696 \times 10^{2}$ $\quad$ $A_9 = 0.23704971 \times 10^{-4}$

$A_5 = 0.36226837 \times 10^{1}$

Temperature (function of enthalpy)

$A_1 = 0.40000290 \times 10^{3}$ $\quad$ $A_6 = 0.86703630 \times 10^{-9}$

$A_2 = 0.41827332 \times 10^{1}$ $\quad$ $A_7 = -0.27042766 \times 10^{-11}$

$A_3 = -0.64799748 \times 10^{-3}$ $\quad$ $A_8 = 0.48670442 \times 10^{-14}$

$A_4 = 0.12160439 \times 10^{-4}$ $\quad$ $A_9 = -0.47242455 \times 10^{-17}$

$A_5 = -0.15484329 \times 10^{-6}$ $\quad$ $A_{10} = 0.19149538 \times 10^{-20}$

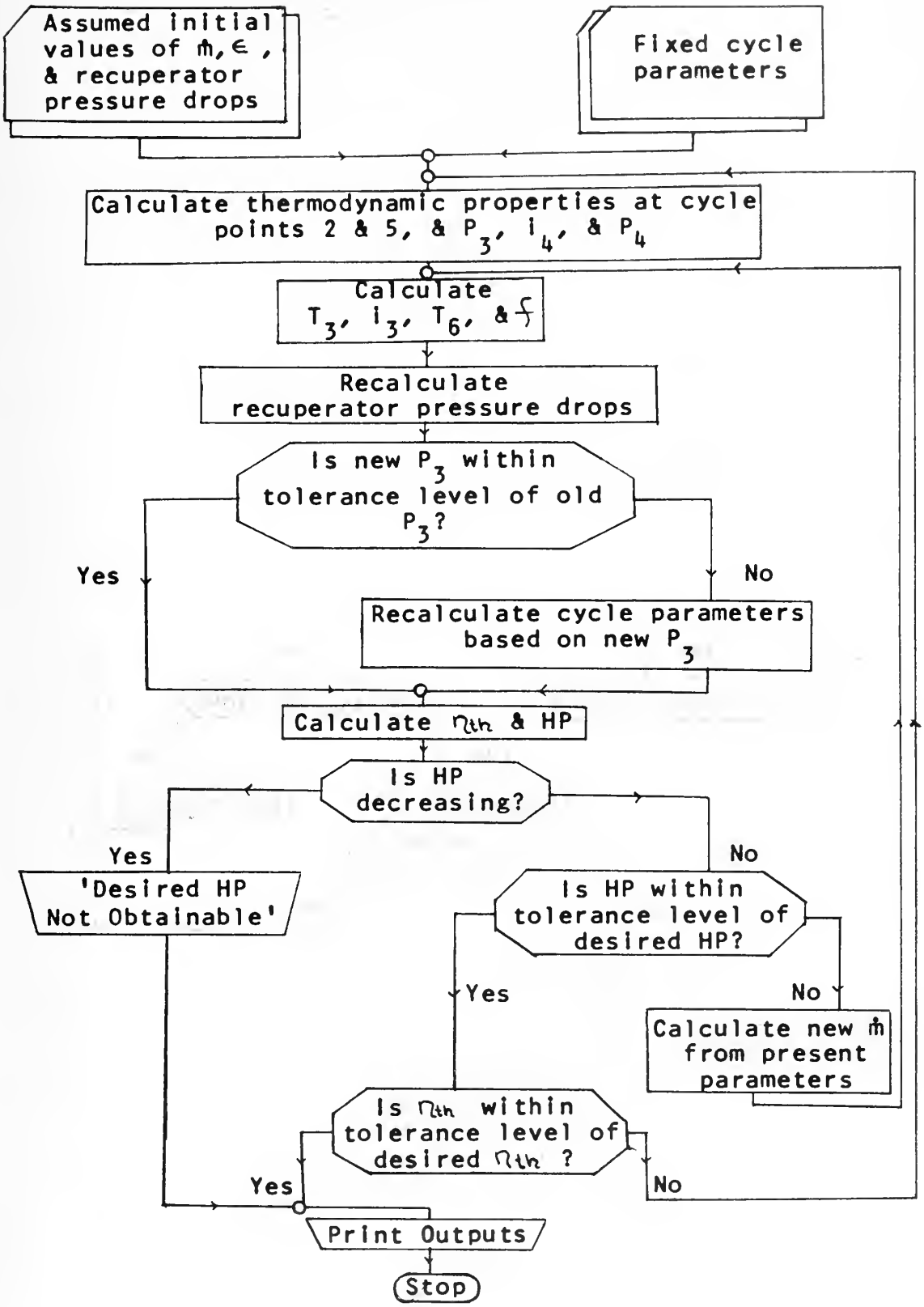

FIGURE 25 PROGRAM FLOW CHART

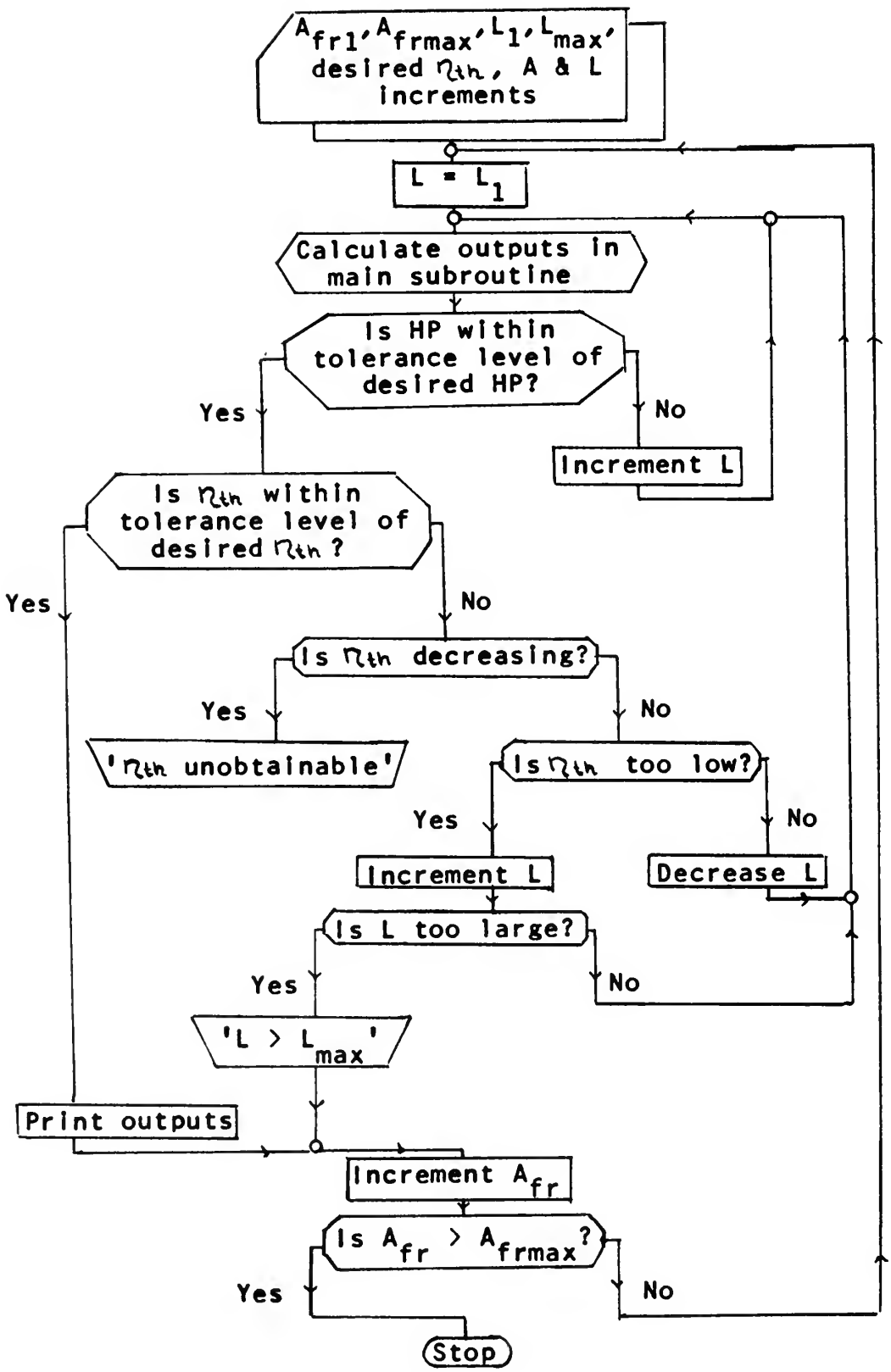

FIGURE 26 OUTPUT III FLOW CHART

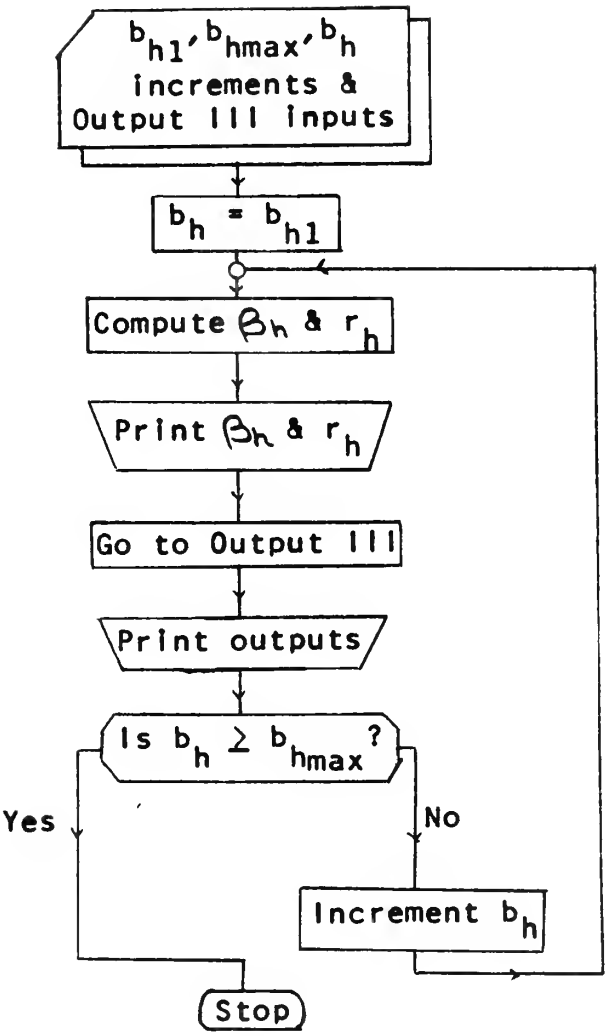

FIGURE 27 OUTPUT VIII FLOW CHART

```
OUTPUT TYPE THREE

  SPECIAL INPUT PARAMETERS
    MINIMUM FRONTAL AREA = 2.300 SQ.FT.        LMIN = 5.350 FT.
    MAXIMUM FRONTAL AREA = 2.400 SQ.FT.        LMAX =20.000 FT.
    FRONTAL AREA INCREMENT = 0.005 SQ.FT.      LINC = 0.005 FT.
    THERMAL EFFICIENCY =0.340
  OUTPUT DESIRED - CORRESPONDING LENGTHS


    DESIRED THERMAL EFFICIENCY NOT OBTAINABLE WITH FRONTAL AREA = 2.300
    MAXIMUM THERMAL EFFICIENCY =0.337 AT A LENGTH OF  5.350 FT.

  HORSEPOWER      THERMAL EFFICIENCY      SPECIFIC FUEL CON      FUEL TO AIR RATIO      MASS FLO RATE
     599.92            0.3372                 0.397                 0.0108               22140.

   TRANSFER UNITS      CMIN/CMAX      REGENERATOR EFFECTIVENESS      AIR SIDE REYNOLDS NO      GAS SIDE REYNOLDS N
        3.00             0.966                 0.759                   4109.                    3751.

   AIR SIDE DELTA P/P      GAS SIDE DELTA P/P      REGENERATOR VOLUME      REGENERATOR WEIGHT      RATIO GAS/AI FRONTAL AREA
        0.009                   0.065                 12.3050                  399.71                    1.292

     P2          P3          P4          P5          T2          T3          T5          T6
    58.89       58.35       57.18       15.75       873.       1487.       1681.       1088.


    FRONTAL AREA = 2.305 SQ.FT.    REQUIRED LENGTH = 5.6800 FT.

  HORSEPOWER      THERMAL EFFICIENCY      SPECIFIC FUEL CON      FUEL TO AIR RATIO      MASS FLO RATE
     599.51            0.3395                 0.394                 0.0106               22279.

   TRANSFER UNITS      CMIN/CMAX      REGENERATOR EFFECTIVENESS      AIR SIDE REYNOLDS NO      GAS SIDE REYNOLDS N
        3.18             0.967                 0.770                   4115.                    3772.

   AIR SIDE DELTA P/P      GAS SIDE DELTA P/P      REGENERATOR VOLUME      REGENERATOR WEIGHT      RATIO GAS/AI FRONTAL AREA
        0.010                   0.069                 13.0924                  425.28                    1.292

     P2          P3          P4          P5          T2          T3          T5          T6
    58.89       58.31       57.15       15.81       873.       1497.       1683.       1079.
```

FIGURE 28 COMPUTER OUTPUT

APPENDIX C

ERROR ANALYSIS

It is a basic fact that all engineering investigations are subject to inaccuracies. As in any other study, a computer analysis is inherently in error due to: (1) the basic assumptions involved to facilitate the problem solution (as neglecting plate heat transfer resistance in equation 4.7) and (2) the approximations made in order to use previously compiled engineering data (as the polynomial curve fittings discussed in Appendix B). A complete examination of all the errors introduced by these factors would be not only time consuming, but quite pointless.

The most significant error in this computer analysis arises from the use of tolerance limits on necessary output parameters and finite increments on input parameters. This investigation necessitates the use of two sets of tolerance levels. The first, Set I, involves a tolerance limit of 3.3% ($0.3389 \leq \eta_{th} \leq 0.3411$) on the desired thermal efficiency of 0.34 and a limit of 0.2% ($599.0 \leq HP \leq 601.0$) on the desired 600 horsepower. Data for these limits is calculated at frontal area increments for the recuperator core of 0.02 sq ft and length increments of 0.01 ft. Further investigation, in the area of optimization, requires tighter tolerances of 1.45% ($0.3395 \leq \eta_{th} \leq 0.3405$) on the thermal efficiency and 0.09% ($599.5 \leq HP \leq 600.5$) on the horsepower. Data for these levels, designated as Set II, is supplied at frontal area increments of 0.005 sq ft and length increments of 0.005 ft. Data from Set I is reproduced in Figures 8 through 14 and

Tables III through IV; Set II data is presented in Figures 15 through 22 and Tables V through VIII.

As there are no performance characteristics available for the majority of recuperator cores investigated in this study, no judgement can be made as to the errors introduced by the computer simulation. An investigation of variations in core parameters as presented in Table VIII, however, yields an idea as to the relative error introduced by the necessary use of finite tolerances and increments.

It should first be noted in Table VIII that three data sets are presented for each core. Set III involves the use of tolerance levels as specified for Set II, with reduced frontal area and length increment magnitudes of 0.002. Variations between Sets II and III are so small that the added computer calculation time introduced with the use of Set III over-rides the slight benefits due to the smaller increments.

Variations in all outputs except dimensional and weight parameters are of such an order that the error in computing these quantities seems negligible. The most noticeable differences between output sets arise in the frontal area and length requirements and the subsequent weight and volume quantities. The effect of tolerance levels on dimensional requirements is more noticeable in Figures 29 and 30.

As may be seen, for any given frontal area, the tighter tolerance of Set II produces a core of greater length than Set I. A comparison of the two plots results in the fact that this effect is more noticeable at larger core spacings. For all cores tested, length variations between sets decrease as frontal areas increase and less core length is required. It is difficult to establish a trend as to the frontal areas of minimum volume cores for the two sets. Although Table VIII indicates

that Set II produces minimum volume cores of greater frontal area than Set I, this effect does not hold for all cores investigated. However, all Set II minimum volume cores of less frontal area than the corresponding Set I minimum volume core require a much greater length than that for the Set I core. Thus, the overall volume and weight trends between cores for each specific set seem to hold.

The most important questions concerning relative error of the analysis have been answered. There is evidently little error in the performance characteristics output. Dimensional comparisons between the two sets result in a maximum difference in length of 0.1 ft for any given frontal area and 0.1 sq ft in area for any minimum volume core. Most important, due to similar trends in the two sets, the data presented may be assumed to provide specific patterns in plate-fin counterflow recuperator core dimensions and weight requirements, while the actual magnitudes presented may be assumed to be within a reasonable range of those which might actually be required.

TABLE VIII

THE EFFECT OF TOLERANCE LIMITS ON MINIMUM VOLUME DIMENSIONS OF SPECIFIC CORES

A_{fr} (sq ft)	L (ft)	V (cu ft)	Wt (lbm)	$\left(\frac{\Delta P}{P}\right)_c$	$\left(\frac{\Delta P}{P}\right)_h$	ϵ	$\dot{m}$ (lbm/hr)	η_{th}	HP (hp)
Core (.125,.225)									
Set I									
2.200	3.565	7.8430	410.38	.025	.060	.774	22452	.3389	599.11
Set II									
2.225	3.585	7.9766	417.37	.024	.059	.774	22419	.3395	599.68
Set III									
2.222	3.588	7.9725	417.16	.024	.059	.775	22441	.3395	600.00
Core (.4,.5)									
Set I									
2.860	8.310	23.767	500.13	.004	.038	.733	21143	.3390	599.19
Set II									
2.885	8.330	24.032	505.72	.004	.038	.734	21139	.3395	599.53
Set III									
2.882	8.338	24.030	505.68	.004	.038	.734	21159	.3395	600.00

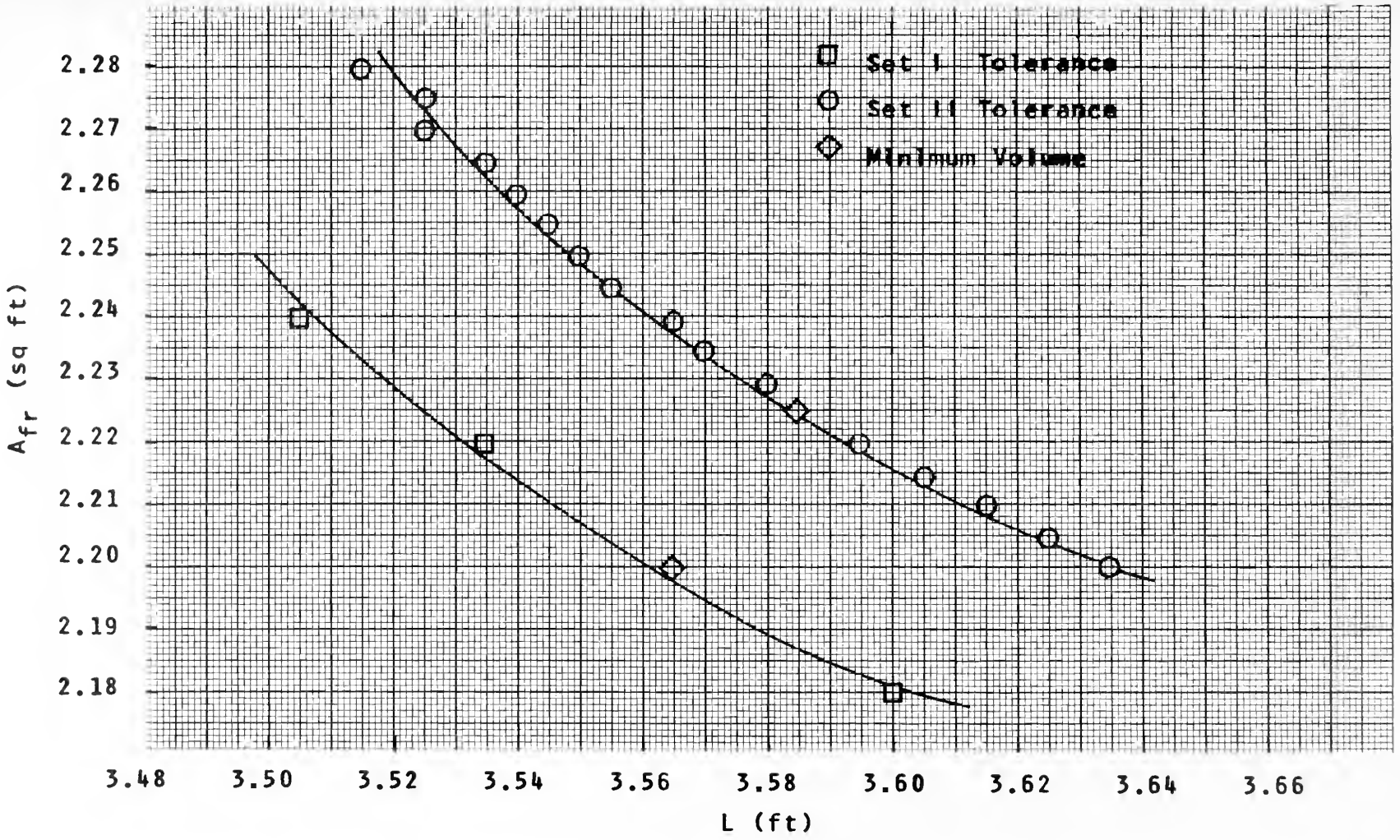

FIGURE 29 EFFECT OF TOLERANCE LIMITS ON (.125,.225) CORE

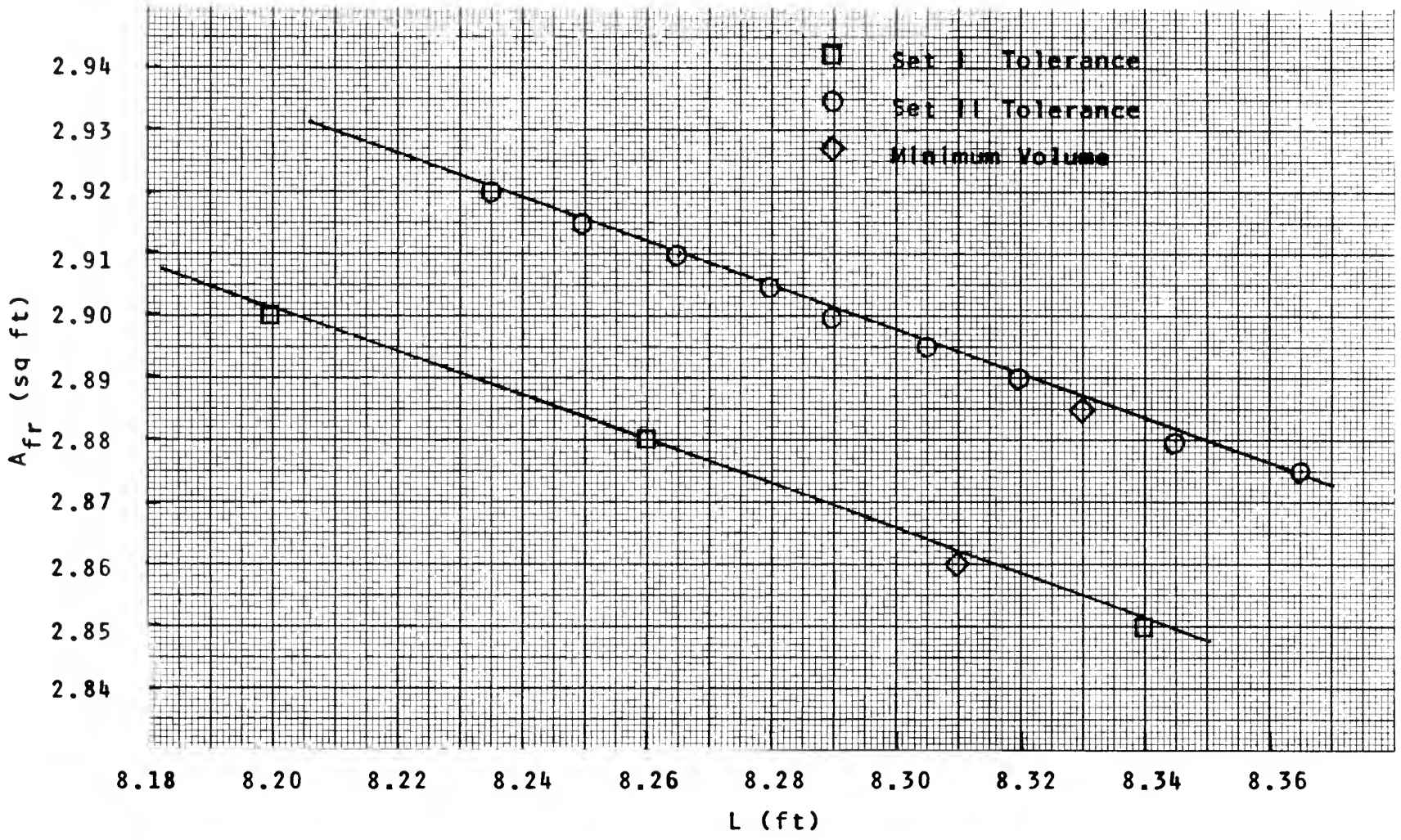

FIGURE 30 EFFECT OF TOLERANCE LIMITS ON (.4,.5) CORE

BIBLIOGRAPHY

1. Carpenter, S. P. Computer Program for Sizing Gas Turbine Counter-flow Recuperators, Master's Thesis, Naval Postgraduate School, Monterey, 1967.

2. Chapman, A. J., Heat Transfer, 2d ed., The Macmillan Company, 1967.

3. Dusinberre, G. M. and Lester, J. C., Gas Turbine Power, 2d ed., International Textbook Company, 1958.

4. Faires, V. M. Thermodynamics, The Macmillan Company, 1962.

5. Howard, C. P., "Thermodynamics and Fundamentals of the Gas Turbine Cycle", and "Cycle Calculations and Variations", Gas Turbine Engineering Handbook, Gas Turbine Publications, Inc., 1966. p 1-28.

6. Howard, C. P., "Heat Exchangers", Gas Turbine Engineering Handbook, Gas Turbine Publications, Inc., 1966. p 183-190.

7. Hryniszak, W., Heat Exchangers, Butterworth's Scientific Publications, 1958.

8. Kays, W. M. and London, A. L., Compact Heat Exchangers, 2d ed., McGraw-Hill Book Company, 1964.

9. London, A. L., "Compact Heat Exchangers", Mechanical Engineering, v. 88, p 47-51, May 1964, p 31-34, June 1964, p 33-35, July 1964.

10. Quan, D., "The Design and Development of the Orenda OT-4 Gas Turbine", Trans. ASME, Journal of Engineering for Power, v. 88, p 117-126, 1966.

INITIAL DISTRIBUTION LIST

		No. Copies
1.	Defense Documentation Center Cameron Station Alexandria, Virginia 22314	20
2.	Library, Code 0212 Naval Postgraduate School Monterey, California 93940	2
3.	Naval Ship Systems Command, Code 2052 Department of the Navy Washington, D. C. 20360	1
4.	Professor P. F. Pucci, Code 59Pc Mechanical Engineering Department Naval Postgraduate School Monterey, California 93940	5
5.	LTJG B. V. Burrow, USN 533 McGilvra Blvd., East Seattle, Washington 98102	2
6.	Mechanical Engineering Department Naval Postgraduate School Monterey, California 93940	2

DOCUMENT CONTROL DATA - R & D

(Security classification of title, body of abstract and indexing annotation must be entered when the overall report is classified)

1. ORIGINATING ACTIVITY *(Corporate author)*
Naval Postgraduate School
Monterey, California 93940

2a. REPORT SECURITY CLASSIFICATION
Unclassified

2b. GROUP

3. REPORT TITLE

The Effect of Recuperator Geometry on a Regenerated Brayton Cycle

4. DESCRIPTIVE NOTES *(Type of report and, inclusive dates)*
Master's thesis; June 1969

5. AUTHOR(S) *(First name, middle initial, last name)*
Barry Vaile Burrow

6. REPORT DATE
June 1969

7a. TOTAL NO. OF PAGES
95

7b. NO. OF REFS
10

8a. CONTRACT OR GRANT NO.

b. PROJECT NO.

c.

d.

9a. ORIGINATOR'S REPORT NUMBER(S)

9b. OTHER REPORT NO(S) *(Any other numbers that may be assigned this report)*

10. DISTRIBUTION STATEMENT

Distribution of this document is unlimited

11. SUPPLEMENTARY NOTES

12. SPONSORING MILITARY ACTIVITY
Naval Postgraduate School
Monterey, California 93940

13. ABSTRACT

A computer simulation of the Brayton cycle is used to develop a design procedure with respect to minimizing volume and weight for the counterflow plate-fin recuperator. Based on the Orenda OT-4 600 horsepower gas turbine, recuperator performance and dimensional characteristics are presented for an idealized equilateral plate-fin recuperator core matrix. The effects of plate spacings varying between 0.1 inches and 0.5 inches on recuperator performance characteristics are presented over a wide range of core frontal areas. Specific trends toward minimum volume and minimum weight plate-fin recuperator cores are discussed in detail.

14 KEY WORDS	LINK A		LINK B		LINK C	
	ROLE	WT	ROLE	WT	ROLE	WT
Gas Turbine						
Regenerated Brayton Cycle						
Recuperator						